

1 Root hair-endophyte stacking (RHESt) in an ancient Afro-Indian crop creates an
2 unusual physico-chemical barrier to trap pathogen(s)

3
4 W. K. Mousa¹, C. Shearer¹, Victor Limay-Rios², C. Ettinger³, J. A. Eisen³, and M.N. Raizada¹

5 ¹Department of Plant Agriculture, University of Guelph, Guelph, ON Canada N1G 2W1

6 ²Department of Plant Agriculture, University of Guelph, Ridgetown Campus, Ridgetown, ON,
7 Canada, N0P 2C0

8 ³University of California Davis Genome Center, Davis, California, USA 95616

9
10 *Author for correspondence:

11 Manish N. Raizada

12 Email: raizada@uoguelph.ca; Phone 1-519-824-4120 x53396; FAX 1-519-763-8933

13

14

15

16

17

18

19 **The ancient African crop, finger millet, has broad resistance to pathogens including the**
20 **toxigenic fungus *Fusarium graminearum*. Here we report the discovery of a novel plant**
21 **defence mechanism, resulting from an unusual symbiosis between finger millet and a root-**
22 **inhabiting bacterial endophyte, M6 (*Enterobacter* sp.). Seed-coated M6 swarms towards**
23 ***Fusarium* attempting to penetrate root epidermis, induces growth of root hairs which then**
24 **bend parallel to the root axis, then forms biofilm-mediated microcolonies, resulting in a**
25 **remarkable, multi-layer root hair-endophyte stack (RHESt). RHESt results in a physical**
26 **barrier that prevents entry and/or traps *F. graminearum* which is then killed. Thus M6**
27 **creates its own specialized killing microhabitat. M6 killing requires c-di-GMP-dependent**
28 **signalling, diverse fungicides and xenobiotic resistance. Further molecular evidence**
29 **suggests long-term host-endophyte-pathogen co-evolution. The end-result of this**
30 **remarkable symbiosis is reduced DON mycotoxin, potentially benefiting millions of**
31 **subsistence farmers and livestock. RHESt demonstrates the value of exploring ancient,**
32 **orphan crop microbiomes.**

33

34 Introduction

35 Finger millet (*Eleusine coracana*) is a cereal crop widely grown by subsistence farmers in
36 Africa and South Asia^{1,2}. Finger millet was domesticated in Western Uganda and Ethiopia
37 around 5000 BC then reached India by 3000 BC³. With few exceptions, subsistence farmers
38 report that finger millet is widely resistant to pathogens including *Fusarium* species^{4,5}. One
39 species of *Fusarium*, *F. graminearum*, causes devastating diseases in crops related to finger
40 millet including maize, wheat and barley, associated with accumulation of the mycotoxin
41 deoxynivalenol (DON) which affects humans and livestock^{6,7}. However, despite its prevalence
42 as a disease-causing agent across cereals, *F. graminearum* is not considered to be an important
43 pathogen of finger millet, suggesting this crop has tolerance to this *Fusarium* species^{4,8}.

44

45 The resistance of finger millet grain to fungal disease has been attributed to high
46 concentrations of polyphenols^{9,10}. However, emerging literature suggests that microbes that
47 inhabit plants without themselves causing disease, defined as endophytes, may contribute to host
48 resistance against fungal pathogens^{11,12}. Endophytes have been shown to suppress fungal
49 diseases through induction of host resistance genes¹³, competition¹⁴, and/or production of anti-
50 pathogenic natural compounds^{15,16}.

51

52 *Fusarium* are ancient fungal species, dating to at least 8.8 million years ago, and their
53 diversification appears to have co-occurred with that of the C4 grasses (which includes finger
54 millet), certainly pre-dating finger millet domestication in Africa¹⁷. Multiple studies have
55 reported the presence of *Fusarium* in finger millet in Africa and India¹⁸⁻²³. A diversity of *F.*

56 *verticillioides* (synonym *F. moniliforme*) has been observed in finger millet in Africa and it has
57 been suggested that the species evolved there¹⁸. These observations suggest the possibility of co-
58 evolution within finger millet between *Fusarium* and millet endophytes. We previously isolated,
59 for the first time, fungal endophytes from finger millet and showed that their natural products
60 have anti-*Fusarium* activity⁴. We could not find reports of bacterial endophytes isolated from
61 finger millet.

62

63 The objectives of this study were to isolate bacterial endophytes from finger millet, assay
64 for anti-*Fusarium* activity and characterize the underlying cellular, molecular and biochemical
65 mechanisms. We report an unusual symbiosis between the host and a root-inhabiting bacterial
66 endophyte.

67

68 **Results**

69 **Isolation, identification and antifungal activity of endophytes**

70 A total of seven bacterial endophytes were isolated from surface-sterilized tissues of finger
71 millet, strains M1 to M7 (Fig. 1a-c and Supplementary Table 1). BLAST searching of the 16S
72 rDNA sequences against Genbank suggested that strains M1 and M6 resemble *Enterobacter* sp.
73 while M2 and M4 resemble *Pantoea* sp., and M3, M5, and M7 resemble *Burkholderia* sp..
74 GenBank accession numbers for strains M1, M2, M3, M4, M5, M6 and M7 are KU307449,
75 KU307450, KU307451, KU307452, KU307453, KU307454, and KU307455, respectively. The
76 16S rDNA sequences for finger millet bacterial endophytes were used to generate a phylogenetic

77 tree (Supplementary Fig.1) using Phylogeny.fr software^{24,25}. Interestingly, five of the seven strains
78 showed anti-fungal activity against *F. graminearum in vitro* (Fig. 1c-d). Strain M6 from millet
79 roots showing the most potent activity and hence was selected for further study including whole
80 genome sequencing, which resulted in a final taxonomic classification (*Enterobacter* sp., strain
81 UCD-UG_FMILLET)²⁶. M6 was observed to inhibit the growth of 5 out of 20 additional crop-
82 associated fungi, including pathogens, suggesting it has a wider target spectrum (Supplementary
83 Table 2). As viewed by electron microscopy, M6 showed an elongated rod shape with a wrinkled
84 surface (Fig. 1e). Following seed coating, GFP-tagged M6 localized to finger millet roots
85 intercellularly and intracellularly (Fig. 1f,g). In addition, colonization of finger millet with M6
86 did not result in pathogenic symptoms (Supplementary Fig. 2). Combined, these results confirm
87 that M6 is an endophyte of finger millet.

88

89 To determine whether strain M6 has anti-*Fusarium* activity *in planta*, related *Fusarium*-
90 susceptible cereals (maize and wheat) were used as model systems (Fig. 1 h-r), since finger
91 millet itself is not reported to be susceptible to *F. graminearum*. Seed-coated GFP-tagged M6
92 was shown to colonize the internal tissues of maize (Fig. 1h) and wheat (Fig. 1n) suggesting it
93 can also behave as an endophyte in these crop relatives. Treatments (combined seed coating and
94 foliar spray) with M6 caused statistically significant ($P \leq 0.05$) reductions in *F. graminearum*
95 disease symptoms in maize (Gibberella Ear Rot, Fig. 1i-l) and wheat (Fusarium Head Blight, Fig.
96 1o-q) ranging from 70 to 90% and 20-30%, respectively in two greenhouse trials, compared to
97 plants treated with *Fusarium* only (yield data in Supplementary Fig. 3a-b; Supplementary Table
98 3). Foliar spraying alone with M6 resulted in more disease reduction compared to seed coating
99 alone, though this effect was not statistically significant, at $P \leq 0.05$ (Supplementary Fig. 3c).

100 Following extended storage to mimic those of African subsistence farmers (ambient temperature
101 and moisture), treatment with M6 resulted in dramatic reductions in DON accumulation, with
102 DON levels declining from ~3.4 ppm to 0.1 ppm in maize, and from 5.5 ppm to 0.2 ppm in
103 wheat, equivalent to 97% and 60% reductions, respectively, compared to plants treated with
104 *Fusarium* only, at $P \leq 0.05$ (Fig. 1m,r and Supplementary Table 4).

105

106 **Microscopic imaging of M6-*Fusarium* interactions in finger millet roots and *in vitro***

107 Since *F. graminearum* has been reported to infect cereal roots²⁷, and since endophyte M6
108 was originally isolated from the same tissue, finger millet roots were selected to visualize
109 potential interactions between M6 and *F. graminearum* (Fig. 2). GFP-tagged M6 was coated
110 onto millet seed. Following germination (Fig. 2a), GFP-M6 showed sporadic, low population
111 density distribution throughout the seminal roots (Fig. 2b). Following inoculation with *F.*
112 *graminearum*, which was visualized using calcofluor staining, GFP-M6 accumulated at sites of
113 attempted entry by *Fusarium*, creating a remarkable, high density layer of microcolonies of M6
114 along the entire root epidermal surface, the rhizoplane (Fig. 2c,d). External to the M6 rhizoplane
115 barrier was a thick mat of root hairs (RH) (Fig. 2c,d). RH number and length were much greater
116 at sites of M6 accumulation compared to the opposite side (Fig. 2c), and M6 was shown *in vitro*
117 to produce auxin (Supplemental Method 1, Supplementary Fig. 4), a known RH-growth
118 promoting plant hormone²⁸. Interestingly, most RH were bent, parallel to the root axis (Fig. 2d).
119 The RH mat appeared to obscure M6 cells, and when observed in a low RH density area (Fig.
120 2e), M6 cells were clearly visible and appeared to attach onto root hairs and engulf *Fusarium*
121 hyphae (Fig. 2f). Imaging at deeper confocal planes below the surface of the RH mat (Fig. 2g,h)

122 revealed that the mat did not consist only of RH, but rather that M6 cells were intercalated
123 between bent RH strands forming an unusual, multi-layer root hair-endophyte stack (RHESt).
124 Within the RHESt, *F. graminearum* hyphae appeared to be trapped (Fig. 2h). By imaging only
125 the M6-*Fusarium* interaction within the RHESt, M6 microcolonies were observed to be
126 associated with breakage of the fungal hyphae (Fig. 2i,j). To confirm that the endophyte actively
127 kills *Fusarium*, Evans blue vitality stain, which stains dead hyphae blue, was used following co-
128 incubation on a microscope slide. The fungal hyphae in contact with strain M6 stained blue and
129 appeared broken (Fig. 3a) in contrast to the control (*F. graminearum* exposed to buffer only)
130 (Fig. 3b). The M6 result was similar to the well known fungicidal activity of the commercial
131 biocontrol agent, *B. subtilis* (Fig. 3c). Combined, these results suggest that M6 cooperates with
132 RH cells to create a specialized killing microhabitat (RHESt) that protects millet roots from
133 invasion by *F. graminearum*.

134

135 Since M6, in the absence of *Fusarium*, was sporadically localized *in planta*, but then
136 accumulated at sites of *Fusarium* hyphae, it was hypothesized that M6 actively seeks *Fusarium*.
137 To test this hypothesis, GFP-tagged M6 and *F. graminearum* were spotted adjacent to one
138 another on a microscope slide coated with agar; as time progressed, M6 was observed to swarm
139 towards *Fusarium* hyphae (Fig. 3d-i), confirming its ability to seek *Fusarium*. Upon finding the
140 pathogen, M6 cells were observed to physically attach onto *F. graminearum* hyphae (Fig. 3g-i).
141 At the endpoint of these interactions, dense microcolonies of M6 were observed to break the
142 hyphae (Fig. 3j). Transmission electron microscopy showed that M6 possesses multiple
143 peritrichous flagella (Fig. 3k). Since this interaction was observed *in vitro*, independent of the
144 host plant, the data show that M6 alone is sufficient to exert its fungicidal activity. To test if the

145 attachments of M6 observed *in vitro* and *in planta* are mediated by biofilm formation, the
146 proteinaceous biofilm matrix stain, Ruby Film Tracer (red), was used *in vitro*. Red staining,
147 indicating biofilm formation, was observed associated with M6 in the absence of *Fusarium* (Fig.
148 3l). In the presence of *F. graminearum*, biofilm was also observed on the hyphal surfaces (Fig.
149 3m). Combined, these results suggest that M6 cells swarm towards *Fusarium* hyphae attempting
150 to penetrate the root epidermis, induces root hair growth and bending, resulting in formation of
151 RHESt within which M6 cells form biofilm-mediated microcolonies which attach, engulf and
152 kill *Fusarium*.

153

154 **Identification of strain M6 genes required for anti-*Fusarium* activity**

155 Since the fungicidal activity of M6 was observed to occur independently of its host plant,
156 M6 was subjected to Tn5 mutagenesis and then candidate Tn5 insertions were screened *in vitro*
157 for loss of fungicidal activity against *F. graminearum*. Out of 4800 Tn5 insertions that were
158 screened in triplicate, sixteen mutants were isolated that resulted in loss or reduction in the
159 diameter of inhibition zones of *F. graminearum* growth (Supplementary Fig. 5a). The mutants
160 that resulted in complete loss of the antifungal activity *in vitro* were validated for loss of anti-
161 *Fusarium* activity *in planta* in two independent greenhouse trials in maize (Supplementary Fig.
162 5b,c), demonstrating the relevance of the *in vitro* results. Rescue of the Tn5-flanking sequences
163 followed by BLAST searching against the whole genome wild type M6²⁶, resulted in the
164 successful identification of 13 candidate genes in 12 predicted operons (Supplementary Table 5
165 and 6). Based on gene annotations and the published literature, four regulatory and/or anti-
166 microbial mutants of interest were selected, complemented (Supplementary Fig. 5d) and

167 subjected to detailed characterization. The selected genes encode two LysR family
168 transcriptional regulators, a diguanylate cyclase, and a colicin V biosynthetic enzyme:

169 **LysR transcription regulator in a phenazine operon (*ewpR-5D7::Tn5*)**

170 *Ewp-5D7::Tn5* resulted in complete loss of the antifungal activity *in vitro* (Supplementary
171 Fig. 5a) and reduction in activity *in planta* (Fig. 4a). The Tn5 insertion was localized to an
172 operon (*ewp*, Fig. 4b) that included tandem paralogs of *phzF* (*ewpF1* and *ewpF2*) (trans-2,3-
173 dihydro-3-hydroxyanthranilate isomerase, EC # 5.3.3.17), a homodimer enzyme that forms the
174 core skeleton of phenazine, a potent anti-fungal compound²⁹. The insertion occurred within a
175 member of the LysR transcriptional regulator family (*ewpR*), which has been previously reported
176 to induce phenazine biosynthesis³⁰. Three lines of evidence suggest the LysR gene is an
177 upstream regulator of the *ewp* operon. First, the genomic organization showed that LysR was
178 transcribed in the opposite direction as the operon. Second, the LysR canonical binding site
179 sequence (TN₁₁A) was observed upstream of the *phzF* (*ewaF*) coding sequences³¹ (Fig. 4b).
180 Finally, real time PCR revealed that the expression of *ewpF1* and *ewpF2* were dramatically
181 down-regulated in the LysR mutant compared to wild type (Fig. 4c). Combined, these results
182 suggest that EwpR is a regulator of phenazine biosynthesis in strain M6 (Fig. 4d). The crude
183 methanolic extract from EwpR-5D7::Tn5 lost anti-*Fusarium* activity *in vitro* in contrast to
184 extracts from wild type M6 or randomly selected Tn5 insertions that otherwise had normal
185 growth rates (Fig. 4e). Anti-*F. graminearum* bioassay guided assay fractionation using extracts
186 from M6 showed two active fractions (A, B) (Fig. 4e-g), each containing a compound with a
187 diagnostic fragmentation pattern of [M+H]⁺=181.0, corresponding to a phenazine nucleus
188 (C₁₂H₈N₂, MW = 180.08)³², and molecular weights (M+Z= 343.3 and 356.3) indicative of
189 phenazine derivatives [griseolutein A (C₁₇H₁₄N₂O₆, MW= 342.3) and D-alanyl-griseolutein

190 (C₁₈H₁₇N₃O₅, MW=355.3), respectively]³³⁻³⁵. Surprisingly, the *ewp* mutant showed a significant
191 reduction in motility (Fig. 4h) and swarming (Fig. 4i) compared to the wild type (Fig. 4j),
192 concomitant with a ~60 % reduction in flagella (Fig. 4k) compared to wild-type (Fig. 3k), loss of
193 attachment to *Fusarium* hyphae (Fig. 4l) compared to wild-type (inset in Fig. 4l), as well as
194 reductions in biofilm formation (Fig. 4m,n). Combined, these results suggest that *ewpR* is
195 required for multiple steps in the anti-fungal pathway of M6 including phenazine biosynthesis.

196

197 **LysR transcriptional regulator in a fusaric acid resistance pump operon (*ewfR-7D5::Tn5*)**

198 *EwfR-5D7::Tn5* resulted in a significant loss of the antifungal activity *in vitro*
199 (Supplementary Fig. 5a). The Tn5 insertion occurred in an operon (*ewf*, Fig. 5a) that included
200 genes that encode membrane proteins required for biosynthesis of the fusaric acid efflux pump
201 including a predicted *fusE*-MFP/HIYD membrane fusion protein and *fusE* (*ewfD* and *ewfE*,
202 respectively) and other membrane proteins (*ewfB*, *ewfH* and *ewfI*)^{36,37}. Fusaric acid (5-
203 butylpyridine-2-carboxylic acid) is a mycotoxin that is produced by *Fusarium* which interferes
204 with bacterial growth and metabolism and alters plant physiology^{38,39}. Bacterial-encoded fusaric
205 acid efflux pumps promote resistance to fusaric acid^{40,41}. Consistent with expectations, *EwfR*-
206 5D7::Tn5 failed to grow on agar supplemented with fusaric acid compared to the wild type (Fig.
207 5b,c). The Tn5 insertion specifically occurred within a member of the LysR transcriptional
208 regulator family (*ewfR*). Similar to *ewpR* above and a previously published fusaric acid
209 resistance operon⁴¹, the regulator was transcribed in the opposite direction as the *ewf* operon,
210 with this genomic organization suggesting that *ewfR* may be an upstream regulator of the operon.
211 Indeed, the LysR canonical binding site sequence (TN₁₁A) was observed upstream of the *ewfB-J*

212 coding sequences³¹ (Fig. 5a). Finally, real time PCR revealed that the expression of *ewfD* and
213 *ewfE* were dramatically downregulated in the LysR mutant compared to wild type (Fig. 5d).
214 Combined, these results suggest that EwfR is a positive regulator of the *ewf* fusaric acid
215 resistance operon in strain M6.

216

217 In addition, the *ewf* mutant showed a significant reduction in motility (Fig. 5e) and
218 swarming (Fig. 5f) compared to the wild type (Fig. 5g), concurrent with a ~30 % reduction in
219 flagella (Fig. 5h) compared to the wild-type (Fig. 3k). The mutant also showed loss of
220 attachment to *Fusarium* hyphae (Fig. 5i) compared to wild-type (inset) and reductions in biofilm
221 formation (Fig. 4j,k). Combined, these results suggest that strain M6 expression of resistance to
222 fusaric acid is a pre-requisite step that enables subsequent anti-fungal steps.

223

224 **Interaction between the phenazine biosynthetic operon (*ewp*) and the fusaric acid** 225 **resistance operon (*ewf*)**

226 The expression of *ewfR* (LysR regulator of fusaric acid resistance) increased two-fold in
227 the presence of *Fusarium* mycelium *in vitro* after 1 h of co-incubation, and tripled after 2 h (Fig.
228 5l). Expression of *ewfR* was also up-regulated by fusaric acid alone (Fig. 5l), demonstrating that
229 the resistance operon is inducible. Fusaric acid has been shown to suppress phenazine
230 biosynthesis through suppression of quorum sensing regulatory genes⁴². Interestingly,
231 expression of the putative LysR regulator of phenazine biosynthesis (*ewpR*, see above) was
232 downregulated by fusaric acid at log phase (2.5-3 h), but only when fusaric acid resistance was
233 apparently lost (*ewfR* mutant) (Fig. 5m) compared to wild type (Fig. 5n), suggesting that fusaric

234 acid normally represses phenazine biosynthesis in M6. These results provide evidence for an
235 epistatic relationship between the two LysR mutants required for the anti-*Fusarium* activity.

236

237 **Diguanylate cyclase (*ewgS*-10A8::Tn5)**

238 *EwgS*-10A8::Tn5 resulted in a significant loss of the antifungal activity *in vitro*
239 (Supplementary Fig. 5a). The Tn5 insertion occurred in a coding sequence encoding diguanylate
240 cyclase (EC 2.7.7.65) (*ewgS*) that catalyzes conversion of 2-guanosine triphosphate to c-di-GMP,
241 a secondary messenger that mediates quorum sensing and virulence traits⁴³ (Fig. 6a). Addition
242 of exogenous c-di-GMP to the growth medium restored the antifungal activity of the mutant
243 (Fig. 6b). Real time PCR showed that *ewgS* is not inducible by *Fusarium* (Fig. 6c). Consistent
244 with its predicted upstream role in regulating virulence traits, the *ewg* mutant showed dramatic
245 losses in motility (Fig. 6d), swarming (Fig. 6e, compared to wild-type Fig. 6f) and flagella
246 formation (~40 % reduction, Fig. 6g compared to wild-type, Fig. 3k). Attachment to *Fusarium*
247 hyphae (Fig. 6h) and biofilm formation (Fig. 6i-j) appeared to have been lost completely.

248

249 **Colicin V production protein (*EwvC*-4B9::Tn5)**

250 *EwvC*-4B9::Tn5 showed significant loss of the antifungal activity *in vitro* (Supplementary
251 Fig. 5a). The Tn5 insertion occurred in a minimally characterized gene required for colicin V
252 production (*ewvC*) orthologous to *cvpA* in *E.coli*⁴⁴. Colicin V is a secreted peptide antibiotic⁴⁵.
253 Consistent with the gene annotation, *EwvC*-4B9::Tn5 failed to inhibit the growth of an *E. coli*
254 strain that is sensitive to colicin V, compared to the wild type (Fig. 7a). Real time PCR showed

255 that the expression of *ewvC* increased 6-fold after co-incubation with *Fusarium* at log phase (Fig.
256 7b). The mutant showed only limited changes in other virulence traits, including reductions in
257 motility (Fig. 7c) and swarming (Fig. 7d, compared to wild-type, Fig. 7e), but with only a ~15%
258 minor reduction in flagella formation (Fig. 7f, compared to wild-type, Fig. 3k), no obvious
259 change in attachment to *Fusarium* hyphae (Fig. 7g), and only a slight reduction in biofilm
260 formation (Fig. 7h,i).

261

262 **Discussion**

263 **RHESt as a novel plant defence mechanism**

264 We hypothesized that the ancient African cereal finger millet hosts endophytic bacteria that
265 contribute to its resistance to *Fusarium*, a pathogenic fungal genus that has been reported to
266 share the same African origin as its plant target. Here, we report that a microbial inhabitant of
267 finger millet (M6) actively swarms towards invading *Fusarium* hyphae, analogous to mobile
268 immunity cells in animals, to protect plant cells that are immobile, confirming a hypothesis that
269 we recently proposed⁴⁶. Endophyte M6 then builds a remarkable physico-chemical barrier
270 resulting from root hair-endophyte stacking (RHESt) at the rhizosphere-root interface that
271 prevents entry and/or traps *Fusarium* for subsequent killing. Mutant and biochemical data
272 demonstrate that the killing activity of M6 requires genes encoding diverse regulatory factors,
273 natural products and xenobiotic resistance. The RHESt consists of two lines of defence, a dense
274 layer of intercalated root hairs and endophyte microcolonies followed by a long, continuous
275 endophyte barrier layer on the root epidermal surface (see summary model, Supplementary Fig.
276 6). RHESt represents a plant defence mechanism that has not been previously captured to the

277 best of our knowledge and is an unusual example of host-microbe symbiosis.

278

279 The epidermal root surface where microbes reside is termed the rhizoplane⁴⁷⁻⁵¹. Soil
280 microbes have previously been reported to form biofilm-mediated aggregates on the rhizoplane
281⁵²⁻⁵⁷ sometimes as part of their migration from the soil to the root endosphere^{48,58} and may
282 prevent pathogen entry^{48,59}. However, here we report that an endophyte, not soil microbe, forms
283 a pathogen barrier on the rhizoplane. The previously reported soil microbes on the rhizoplane are
284 thought to take advantage of nutrient-rich root exudates⁵⁹, whereas RHESt is a *de novo*,
285 inducible structure that only forms in the presence of *Fusarium* in coordination with root hairs.

286

287 M6 creates its own specialized killing microhabitat by inducing growth of local root hairs
288 which are then bent to form the RHESt scaffold, likely mediated by biofilm formation and
289 attachment. *In vitro*, we observed that M6 synthesizes auxin (IAA), a hormone known to
290 stimulate root hair growth⁶⁰ and that can be synthesized by microbes⁶¹. Root hair bending
291 associated with RHESt might be an active process, similar to rhizobia-mediated root hair curling
292⁶², or an indirect consequence of micro-colonies attachment to adjacent root hairs.

293

294 **Regulatory signals within the anti-fungal pathway**

295 Some of the mutants caused pleiotropic phenotypes, including loss of swarming,
296 attachment and/or biofilm formation, which was a surprising result. These mutants included the
297 transcription factors associated with operons for phenazine biosynthesis, fusaric acid resistance,
298 as well as formation of c-di-GMP. One interpretation of these results is that the underlying
299 genes help to regulate the early steps of the anti-fungal RHESt pathway. Indeed, phenazines have

300 been reported to act as signalling molecules that regulate the expression of hundreds of genes
301 including those responsible for motility and defense⁶³. Our results showed an epistatic
302 relationship between the two transcription factors regulating phenazine biosynthesis and fusaric
303 acid resistance, with the latter required for the former (Fig. 5m,n), suggesting that the pleiotropic
304 phenotypes observed in the fusaric acid resistance regulatory mutant may have been mediated by
305 a reduction in phenazine signaling. Finally, c-di-GMP as a sensor of the environment and
306 population density^{64,65}, and a secondary messenger⁶⁶ involved in transcriptional regulation of
307 genes encode virulence traits such as motility, attachment, and biofilm formation^{43,64,66-68}, all
308 activities that would be logically required for the RHESt-mediated anti-fungal pathway. Genome
309 mining of strain M6 also revealed the presence of a biosynthetic cluster for 2, 3 butanediol which
310 is a hormone known to elicit plant defences⁶⁹. Production of 2, 3 butanediol was confirmed by
311 LC-MS analysis (Supplementary Fig. 7a). Butanediol is thus a candidate signalling molecule for
312 M6-millet cross-talk.

313

314 **Fungicidal compounds required for M6 killing activity**

315 In addition to RHESt formation, we gained evidence that bacterial endophyte M6 evolved
316 multiple biochemical strategies to actively break and kill *Fusarium* hyphae (Fig. 2j and Fig. 3a,j)
317 involving diverse classes of natural products, including phenazines, colicin V, chitinase and
318 potentially other metabolites.

319 *Phenazines*: Phenazines are heterogeneous nitrogenous compounds produced exclusively by
320 bacteria⁷⁰. Phenazines exhibit potent antifungal activity, in particular against soil pathogens
321 including *Fusarium* species⁷¹⁻⁷³. Here M6 was observed to produce at least two distinct

322 phenazines, D-alanyl-griseolutein and griseolutein A which previously shown to have anti-
323 microbial activities⁷⁴. Phenazines lead to the accumulation of reactive oxygen species in target
324 cells, due to their redox potential^{75,76}. Phenazines were also reported to induce host resistance⁷⁷.
325 For bacteria to survive inside a biofilm, where oxygen diffusion is limited, molecules with high
326 redox potential such as phenazines are required⁷⁸⁻⁸². Furthermore, the redox reaction of
327 phenazine releases extracellular DNA which enhances surface adhesion and cellular aggregation
328 of bacteria to form a biofilm⁸³⁻⁸⁸. Consistent with these roles, phenazines are known to be
329 produced inside biofilms⁷⁸, and are required for biofilm formation⁸⁹, which might explain the
330 diminished biofilm formation observed with the phenazine-associated LysR mutant. Since M6
331 was observed to produce biofilm around its fungal target (Fig. 3m) which is killed within RHESt
332 (Fig. 2j), phenazines may be part of the killing machinery.

333 *Colicin V*: An exciting observation from this study is that colicin V also appears to be required
334 for the fungicidal activity of strain M6 (Fig. 7). Colicin V is a small peptide antibiotic belonging
335 to the bacteriocin family which disrupts the cell membrane of pathogens resulting in loss of
336 membrane potential⁹⁰. Bacteriocins are generally known for their antibacterial activities⁹¹.
337 Indeed, we could find only one previous report of colicin V having anti-fungal activity⁹². Our
338 results suggest that this compound may target a wider spectrum of pathogens than previously
339 thought.

340 *Chitinase*: A Tn5 insertion in a gene (*ewc-3H2::Tn5*) encodes chitinase (EC 3.2.1.14), also
341 resulted in a significant loss of the antifungal activity (Supplementary Fig. 5a). The mutant
342 shows a significant reduction in production of chitinase *in vitro*, compared to wild type M6
343 (Supplementary Fig. 7b). Chitinase exerts its antifungal activity by hydrolyzing chitin, a
344 principle component of the fungal cell wall^{93,94}.

345 *Other putative M6 anti-fungal metabolites:* Two additional putative Tn5 mutants suggest that
346 other metabolites may be involved in the anti-*Fusarium* activity of strain M6 within the RHESt,
347 specifically phenylacetic acid (PAA) and P-amino-phenyl-alanine antibiotics (PAPA). The
348 requirement for PAA was suggested by a mutant in phenylacetic acid monooxygenase which
349 resulted in loss of anti-*Fusarium* activity (m2D7, Supplementary Fig. 5a). This enzyme catalyzes
350 the biosynthesis of hydroxy phenylacetic acid, derivatives of which have been shown to act as
351 anti-fungal compounds^{95,96}. In an earlier report, an *Enterobacter* sp. that was used to control
352 *Fusarium* dry rot during seed storage⁹⁷ was shown to require phenylacetic acid, indole-3-acetic
353 acid (IAA) and tyrosol⁹⁶. In addition to PAA implicated here by the Tn5 mutant, wild type strain
354 M6 was shown to produce IAA *in vitro* (Supplementary Fig. 4).

355 The requirement for PAPA was suggested by a putative mutant (m15A12, Supplementary Fig.
356 5a) which disrupted a gene encoding a permease transport protein that is a part of an operon
357 responsible for biosynthesis of PAPA and 3-hydroxy anthranilates. PAPA is the direct precursor
358 of well known antibiotics including chloramphenicol and obaflourin⁹⁸⁻¹⁰⁰.

359

360 **M6-*Fusarium*-millet co-evolution and the fusaric acid-phenazine arms race**

361 Molecular and biochemical data suggest that the anti-fungal activity of M6 requires diverse
362 classes of anti-fungal natural products (phenazine metabolites, colicin V peptide antibiotic,
363 chitinase enzyme). We previously demonstrated that finger millet also hosts fungal endophytes
364 that secrete complementary anti-*F. graminearum* natural products including polyketides and
365 alkaloids⁴. These observations, combined with loss of function mutants from this study that
366 demonstrate that no single anti-fungal mechanism is sufficient for M6 to combat *Fusarium*,

367 suggests that the endophytic community of finger millet and *Fusarium* have been engaged in a
368 step-by-step arms race that resulted in the endophytes having a diverse weapons arsenal,
369 presumably acting within RHESt. Consistent with this interpretation, mutant analysis showed
370 that the anti-fungal activity of M6 requires a functional operon that encodes resistance to the
371 *Fusarium* mycotoxin, fusaric acid. Furthermore, our results show a novel epistatic regulatory
372 interaction between the fusaric acid resistance and phenazine pathways, wherein an M6-encoded
373 LysR activator of fusaric acid resistance prevents fusaric acid from suppressing expression of the
374 M6-encoded LysR regulator of phenazine biosynthesis (Fig. 5m). Fusaric acid has previously
375 been shown to interfere with quorum sensing-mediated biosynthesis of phenazine⁴². We propose
376 that the phenazine-fusaric acid arms race provides a molecular and biochemical paleontological
377 record that M6 and *Fusarium* co-evolved.

378

379 We show how this tripartite co-evolution likely benefits subsistence farmers not only by
380 suppressing *Fusarium* entry and hence disease in plants, but also in seeds after harvest.
381 Specifically, under poor seed storage conditions that mimic those of subsistence farmers, M6
382 caused dramatic reductions in contamination with DON (Fig. 1m,r), a potent human and
383 livestock mycotoxin. Hence, in the thousands of years since ancient crop was domesticated,
384 farmers may have been inadvertently selecting for the physico-chemical RHESt barrier activity
385 of endophyte M6, simply by selecting healthy plants and their seeds. We have shown here that
386 the benefits of M6 are transferable to two of the world's most important modern crops, maize
387 and wheat (Fig. 1i,o), which are severely afflicted by *F. graminearum* and DON. In addition to
388 *F. graminearum*, M6 inhibited the growth of five other fungi including two additional *Fusarium*
389 species (Supplementary Table 2), suggesting that RHESt-mediated plant defence may contribute

390 to the broad spectrum pathogen resistance of finger millet reported by subsistence farmers.
391 Despite its importance, finger millet is a scientifically neglected crop ^{1,2}. Our study suggests the
392 value of exploring microbiome--host interactions of other scientifically neglected, ancient crops.

393

394 **Methods**

395 **Isolation, identification and antifungal activity of endophytes**

396 Finger millet seeds originating from Northern India were grown on clay Turface in the
397 summer of 2012 according to a previously described method ⁴. Tissue pool sets (3 sets of: 5
398 seeds, 5 shoots and 5 root systems from pre-flowering plants) were surface sterilized following a
399 standard protocol ⁴. Surface sterilized tissues were ground in LB liquid medium in a sterilized
400 mortar and pestle, then 50 µl suspensions were plated onto 3 types of agar plates (LB, Biolog
401 Universal Growth, and PDA media). Plates were incubated at 25°C, 30°C and 37°C for 1-3 days.
402 A total of seven bacterial colonies (M1-M7) were purified by repeated culturing on fresh media.
403 For molecular identification of the isolated bacterial endophytes, PCR primers (Supplemental
404 Table 7) were used to amplify and sequence 16S rDNA as previously described ⁷, followed by
405 best BLAST matching to GenBank. 16S rDNA sequences were deposited into GenBank.
406 Scanning electron microscopy imaging was used to phenotype the candidate bacterium as
407 previously described ⁷ using a Hitachi S-570 microscope (Hitachi High Technologies, Tokyo,
408 Japan) at the Imaging Facility, Department of Food Science, University of Guelph.

409

410 To test the antifungal activity of the isolated endophytes against *F. graminearum*, agar

411 diffusion dual culture assays were undertaken in triplicate¹⁰¹. Nystatin (Catalog #N6261, Sigma
412 Aldrich, USA) and Amphotericin B (Catalog #A2942, Sigma Aldrich, USA) were used as
413 positive controls at 10 µg/ml and 5µg/ml, respectively, while the negative control was LB
414 medium. Using a similar methodology, additional anti-fungal screening was conducted using the
415 Fungal Type Culture Collection at Agriculture and Agrifood Canada, Guelph, ON
416 (Supplementary Table 2).

417

418 **Microscopy imaging**

419 ***In planta* colonization of the candidate anti-fungal endophyte M6**

420 In order to verify the endophytic behaviour of the candidate anti-fungal bacterium M6 in
421 maize, wheat and millet, the bacterium was subjected to tagging with green fluorescent protein
422 (GFP) (vector pDSK-GFPuv)¹⁰¹ and *in planta* visualization using confocal scanning microscopy
423 as previously described¹⁰¹ at the Molecular and Cellular Imaging Facility, University of Guelph,
424 Canada.

425

426 ***In vitro* interaction using light microscopy**

427 Both the fungus and bacterium M6 were allowed to grow in close proximity to each other
428 overnight on microscope slides coated with a thin layer of PDA as previously described¹⁰¹.
429 Thereafter, the fungus was stained with the vitality stain, Evans blue which stains dead hyphae
430 blue. The positive control was a commercial biological control agent (*Bacillus subtilis* QST713,
431 Bayer CropScience, Batch # 00129001) (100 mg/10 ml). Pictures were captured using a light
432 microscope (BX51, Olympus, Tokyo, Japan).

433 ***In vitro* and *in planta* interactions using confocal microscopy**

434 All the experiments were conducted using a Leica TCS SP5 confocal laser scanning
435 microscope at the Molecular and Cellular Imaging Facility at the University of Guelph, Canada.

436 To visualize the interactions between endophyte M6 and *F. graminearum* inside finger
437 millet, finger millet seeds were surface sterilized and coated with GFP-tagged endophyte, and
438 then planted on sterile Phytigel based medium in glass tubes, each with 4-5 seeds. Phytigel
439 medium was prepared as previously described⁴. At 14 days after planting, finger millet seedlings
440 were inoculated with *F. graminearum* (50 µl of a 48 h old culture grown in potato dextrose
441 broth) and incubated at room temperature for 24 h. The control consisted of seedlings incubated
442 with potato dextrose broth only. There were three replicate tubes for each treatment. Thereafter,
443 roots were stained with calcofluor florescent stain (catalog #18909, Sigma-Aldrich), which stains
444 chitin blue, following the manufacturer's protocol, and scanned.

445

446 To visualize the attachment of bacterium M6 to fungal hyphae, GFP-tagged M6 and *F.*
447 *graminearum* were inoculated overnight at 30°C on microscope slides covered with a thin layer
448 of PDA. Thereafter, the fungal hyphae was stained with calcofluor and examined. The same
449 protocol was employed to test if this recognition was disrupted in the Tn5 mutants.

450

451 To visualize biofilm formation by bacterium M6, GFP-tagged M6 were incubated on
452 microscope slides for 24 h at 30°C. The biofilm matrix was stained with FilmTracer™ SYPRO®

453 Ruby Biofilm Matrix Stain (F10318) using the manufacturer's protocol and then examined. The
454 same protocol was employed to test if the biofilm was disrupted in Tn5 mutants.

455

456 **Suppression of *F. graminearum* in planta and accumulation in storage**

457 Bacterium M6 was tested *in planta* for its ability to suppress *F. graminearum* in two
458 susceptible crops, maize (hybrid P35F40, Pioneer HiBred) and wheat (Quantum spring wheat,
459 C&M Seeds, Canada), in two independent greenhouse trials as previously described for maize
460 ¹⁰¹, with modifications for wheat (Supplemental Method 2). ELISA analysis was conducted to
461 test the accumulation of DON in seeds after 14 months of storage in conditions that mimic those
462 of African subsistence farmers (temperature ~18-25°C, with a moisture content of ~40-60%) as
463 previously described ¹⁰¹. Control treatments consisted of plants subjected to pathogen inoculation
464 only, and plants subjected to pathogen inoculation followed by prothioconazole fungicide
465 spraying (PROLINE® 480 SC, Bayer Crop Science). Results were analyzed and compared using
466 Mann-Whitney t-tests ($P \leq 0.05$).

467

468 **Transposon mutagenesis, gene rescues and complementation**

469 To identify the genes responsible for the antifungal activity, Tn5 transposon mutagenesis
470 was conducted using EZ-Tn5 <R6Kγori/KAN-2>Tnp Transposome™ kit (catalog #TSM08KR,
471 Epicentre, Madison, USA) according to the manufacturer's protocol. The mutants were screened
472 for loss of anti-*Fusarium* activity using the agar dual culture method compared to wild type.
473 Insertion mutants that completely lost the antifungal activity *in vitro* were further tested for loss

474 of *in planta* activity using maize as a model in two independent greenhouse trials (same protocol
475 as described above). The sequences flanking each candidate Tn5 insertion mutant of interest
476 were identified using plasmid rescues according to the manufacturer's protocol (Supplemental
477 Method 3). The rescued gene sequences were BLAST searched against the whole genome
478 sequence of bacterium M6²⁶. To test if the candidate genes are inducible by *F. graminearum* or
479 constitutively expressed, real-time PCR analysis was conducted using gene specific primers
480 (Supplemental Method 4). Operons were tentatively predicted using FGENESB¹⁰² from
481 Softberry Inc. (USA). Promoter regions were predicted using PePPER software (University of
482 Groningen, The Netherlands)¹⁰³. In order to confirm the identity of the genes discovered by Tn5
483 mutagenesis, each mutant was complemented with the corresponding predicted wild type coding
484 sequence which was synthesized (VectorBuilder, Cyagen Biosciences, USA) using a pPR322
485 vector backbone (Novagen) under the control of the T7 promoter. Two microlitres of each
486 synthesized vector was electroporated using 40 µl electro competent cells of the corresponding
487 mutant. The transformed bacterium cells were screened for gain of the antifungal activity against
488 *F. graminearum* using the dual culture assay as described above.

489

490 **Mutant phenotyping**

491 *Transmission electron microscopy (TEM)*: To phenotype the candidate mutants, TEM imaging
492 was conducted. Wild type strain M6 and each of the candidate mutants were cultured overnight
493 in LB medium (37°C, 250 rpm). Thereafter, 5 µl of each culture were pipetted onto a 200-mesh
494 copper grid coated with carbon. The excess fluid was removed onto a filter, and the grid was
495 stained with 2% uranyl acetate for 10 sec. Images were taken by a F20 G2 FEI Tecnai

496 microscope operating at 200 kV equipped with a Gatan 4K CCD camera and Digital Micrograph
497 software at the Electron Microscopy Unit, University of Guelph, Canada.

498

499 *Motility assay:* Wild type or mutant strains were cultured overnight in LB medium (37°C, 225
500 rpm). The OD₅₉₅ for each culture was adjusted to 1.0, then 15 µl of each culture were spotted on
501 the center of a semisolid LB plates (0.3% agar) and incubated overnight (37°C, no shaking).
502 Motility was measured as the diameter of the resulting colony. There were ten replicates for each
503 culture. The entire experiment was repeated independently.

504

505 *Swarming test:* To examine the ability of the strains to swarm and form colonies around the
506 fungal pathogen, *in vitro* interaction/light microscopy imaging was conducted. Wild type M6 and
507 each mutant were incubated with *F. graminearum* on microscope slides covered with PDA (as
508 described above). *F. graminearum* hyphae was stained with lactophenol blue solution (catalog
509 #61335, Sigma-Aldrich) then examined under a light microscope (B1372, Axiophot, Zeiss,
510 Germany) using Northern Eclipse software.

511

512 *Biofilm spectroscopic assay:* To test the ability of the strains to form biofilms, the strains were
513 initially cultured overnight in LB medium (37°C and 250 rpm), and adjusted to OD₆₀₀ of 0.5.
514 Cultures were diluted in LB (1:100), thereafter, 200 µl from each culture were transferred to a 96
515 well microtitre plate (3370, Corning Life Sciences, USA) in 6 replicates. The negative control
516 was LB medium only. The microtitre plate was incubated for 2 days at 37°C. The plate was

517 emptied by aspiration and washed three times with sterile saline solution. Adherent cells were
518 fixed with 200 μ l of 99% methanol for 15 min then air dried. Thereafter, 200 μ l of 2% crystal
519 violet (94448, Sigma) were added to each well for 5 min then washed with water, and left to air
520 dry. Finally, 160 μ l of 33% (v/v) glacial acetic acid were added to each well to solubilise the
521 crystal violet stain. The light absorption was read by a spectrophotometer (SpectraMax plus 348
522 microplate reader, Molecular Devices, USA) at 570 nm¹⁰⁴. The entire experiment was repeated
523 independently.

524

525 *Fusaric acid resistance:* To test the ability of M6 wild type or *EwfR::Tn5* to resist fusaric acid,
526 the strains were allowed to grow on LB agar medium supplemented with different concentrations
527 of fusaric acid (0.01, 0.05 and 0.1%, catalog #F6513, Sigma Aldrich) as previously reported¹⁰⁵.

528

529 *c-di-GMP chemical complementation:* To test if the Tn5 insertion in the predicted guanylate
530 cyclase gene could be complemented by exogenous c-di-GMP, M6 wild type or *EwgC::Tn5*
531 strains were grown on LB agar medium supplemented with c-di-GMP (0.01 or 0.02 mg/ml)
532 (Catalogue # TLRL-CDG, Cedarlane). After 24 h, the agar diffusion method was used to test for
533 antifungal activity.

534

535 *Colicin V assay:* To verify that the Tn5 insertion in the predicted colicin V production gene
536 caused loss of colicin V secretion, M6 wild type or *EwvC-4B9::Tn5* strains were inoculated as

537 liquid cultures ($OD_{600} = 0.5$) into holes created in LB agar medium pre-inoculated after cooling
538 with an *E.coli* strain sensitive to colicin V (MC4100, ATCC 35695)⁹⁰.

539

540 **Biochemical and enzymatic assays**

541 *Detection of anti-fungal phenazine derivatives:* For phenazine detection, bio-guided fractionation
542 combined with LC-MS analysis was undertaken. Wild type M6 or mutant bacterial strains were
543 grown for 48 h on Katznelson and Lochhead liquid medium¹⁰⁶, harvested by freeze drying, then
544 the lyophilized powder from each strain was extracted by methanol. The methanolic extracts
545 were tested for anti-*Fusarium* activity using the agar diffusion method as described above. The
546 extracts were dried under vacuum and dissolved in a mixture of water and acetonitrile then
547 fractionized over a preparative HPLC C18 column (Nova-Pak HR C18 Prep Column, 6 μ m, 60
548 Å, 25 x 100 mm prepack cartridge, part # WAT038510, Serial No 0042143081sp, Waters Ltd,
549 USA). The solvent system consisted of purified water (Nanopure, USA) and acetonitrile (starting
550 at 99:1 and ending at 0:100) pumped at a rate of 5 ml/min. The eluted peaks were tested for anti-
551 *Fusarium* activity. Active fractions were subjected to LC-MS analysis. Each of the active
552 fractions was run on a Luna C18 column (Phenomenex Inc, USA) with a gradient of 0.1% formic
553 acid in water and 0.1% formic in acetonitrile. Peaks were analyzed by mass spectroscopy
554 (Agilent 6340 Ion Trap), ESI, positive ion mode. LC-MS analysis was conducted at the Mass
555 Spectroscopy Facility, McMaster University, ON, Canada.

556

557 *GC-MS to detect production of 2,3 butanediol:* To detect 2,3 butanediol, wild type strain M6 was
558 grown for 48 h on LB medium. The culture filtrate was analyzed by GC-MS (Mass Spectroscopy

559 Facility, McMaster University, ON, Canada) and the resulting peaks were analyzed by searches
560 against the NIST 2008 database.

561

562 *Chitinase assay:* Chitinase activity of wild type strain M6 and the putative chitinase Tn5 mutant
563 was assessed using a standard spectrophotometric assay employing the Chitinase Assay Kit
564 (catalog #CS0980, Sigma Aldrich, USA) according to the manufacturer's protocol. There were
565 three replicates for each culture, and the entire experiment was repeated independently.

566

567 **Figures legends**

568 **Figure 1| Isolation, identification and antifungal activity of endophytes. a**, Picture showing
569 finger millet grain head. **b**, Mixed culture of endophytes isolated from finger millet. **c**,
570 Quantification of the inhibitory effect of finger millet endophytes or fungicide controls on the
571 growth of *F. graminearum in vitro*. For these experiments, n=3. **d**, M6 endophyte suppresses the
572 growth of *F. graminearum* hyphae (white) using the dual culture method. **e**, Imaging of M6
573 viewed by scanning electron microscopy. **f-g**, GFP-tagged M6 inside roots of finger millet
574 viewed by scanning confocal microscopy. **h**, GFP-tagged M6 inside roots of maize (stained with
575 propidium iodide). **i**, Effect of M6 treatment on suppression of *F. graminearum* disease in maize
576 in two greenhouse trials. **j-l**, (left to right) Representative ears from M6, fungicide and *Fusarium*
577 only treatments. **m**, Effect of M6 or controls on reducing DON mycotoxin contamination in
578 maize during storage following the two greenhouse trials. **n**, GFP-tagged M6 inside roots of
579 wheat viewed by confocal microscopy. **o**, Effect of M6 treatment on suppression of *F.*
580 *graminearum* disease in wheat in two greenhouse trials. **p**, Picture of a healthy wheat grain. **q**,

581 Picture of an infected wheat grain. **r**, Effect of M6 or controls on reducing DON mycotoxin
582 contamination in wheat during storage following the two greenhouse trials. Scale bars in all
583 pictures equal 5 μm . For greenhouse disease trials, n=20 for M6 and n=10 for the controls. For
584 DON quantification, n=3 pools of seeds. The whiskers (**i**, **o**) indicate the range of data points.
585 The error bars (**c**, **m**, **q**) indicate the standard error of the mean. For all graphs, letters that are
586 different from one another indicate that their means are statistically different ($P \leq 0.05$).

587

588 **Figure 2| Confocal imaging of m6-*fusarium* interactions in finger millet roots.** **a**, Picture of
589 millet seedling showing primary root (PR) zone used for confocal microscopy. **b**, Control
590 primary root that was seed coated with GFP-M6 (green) but not infected with *F. graminearum*.
591 As a control, the tissue was stained with fungal stain calcofluor to exclude the presence of other
592 fungi. Root following seed coating with GFP-tagged endophyte M6 (M6, green) following
593 inoculation with *F. graminearum* (Fg, purple blue, calcofluor stained) showing interactions with
594 root hairs (RH, magenta, lignin autofluorescence). **c-d**, Low (**c**) and high (**d**) magnifications to
595 show the dense root hair and endophyte barrier layers. **e-f**, Low (**e**) and high (**f**) magnifications at
596 the edge of the barrier layers. **g-h**, Low (**g**) and high (**h**) magnifications in a deeper confocal
597 plane of the root hair layer shown in (**d**) showing root hair endophyte stacking (RHESt) with
598 trapped fungal hyphae. **i-j**, Low (**i**) and high (**j**) magnifications of the interactions between M6
599 (green) and *F. graminearum* in the absence of root hair-lignin autofluorescence, showing
600 breakage of fungal hyphae.

601

602 **Figure 3| Behavior and interactions of endophyte m6 and *f. graminearum* in vitro on**
603 **microscope slides. a-c**, Light microscopy of interactions between *F. graminearum* (Fg) and M6
604 following staining with Evans blue, which stains dead hyphae blue. Shown are (a) Fg following
605 overnight co-incubation with M6, (b) Fg, grown away from M6 (control), and (c) Fg following
606 overnight co-incubation with a commercial biological control agent. **d-i**, Time course to
607 illustrate the swarming and attachment behaviour of GFP-tagged M6 (green) to Fg (blue,
608 calcofluor stained) viewed at 0.5 h, 1.5 h, 3 h, 6 h, 6 h (close-up) and 8 h following co-
609 incubation, respectively. Fg and M6 shown in (d) and (e) were inoculated on the same slide
610 distal from one another at the start of the time course but digitally placed together for these
611 illustrations. **j**, M6 shown breaking Fg hypha. **k**, Transmission electron microscope picture of
612 M6 showing its characteristic flagella. **(l-m)** Biofilm formed by M6 as viewed by staining with
613 Ruby film tracer (red) in the (l) absence of Fg or (m) presence of Fg.

614

615 **Figure 4 | Characterization of phenazine mutant *ewpR*-5D7::Tn5. a**, Effect of M6 mutant
616 strain *ewpR* on suppression of *F. graminearum* (Fg) in maize compared to wild type M6 and Fg-
617 only control, with corresponding, representative maize ear pictures. **b**, Genomic organization of
618 the predicted phenazine biosynthetic operon showing the position of the Tn5 insertion and
619 putative LysR binding site within the promoter (P). **c**, Quantitative real time PCR (qRT-PCR)
620 gene expression of the two core phenazine genes (*ewpF1* and *ewpF2*) in wild type M6 (+) and
621 the mutant (-) (*ewpR*). **d**, Illustration of the phenazine biosynthetic pathway. **e**, Agar diffusion
622 assay showing the inhibitory effect of different methanol extracts on the growth of Fg from wild
623 type M6, two wild type fractions (FrA, FrB), the *ewpR* mutant (mutant), a random Tn5 insertion
624 or buffer. **f-g**, Mass spectroscopy analysis of putative phenazine derivatives in wild type M6

625 fractions A and B. **h**, Quantification of *ewpR*⁻ mutant strain (M) motility compared to wild type
626 M6 (W), with representative pictures (inset) of motility assays on semisolid agar plates. **i-j**, Light
627 microscopy image showing loss of swarming and colony formation of (**i**) *ewpR*⁻ mutant strain
628 around Fg hyphae stained with lactophenol blue, compared to (**j**) wild type M6. **k**, Electron
629 microscopy image of *ewpR*⁻ mutant strain. **l**, Confocal microscopy image showing attachment
630 pattern of GFP-tagged *ewpR*⁻ mutant strain (green) to Fg hyphae stained with calcofluor stain,
631 compared to wild type M6 (inset). **m**, Confocal microscopy image showing reduced
632 proteinaceous biofilm matrix stained with Ruby film tracer (red) associated with GFP-tagged
633 *ewpR*⁻ mutant strain compared to wild type M6 (inset). **n**, Spectrophotometric quantification of
634 biofilm formation associated with wild type M6 compared to the *ewpR*⁻ mutant strain, with
635 representative biofilm assay well pictures (left and right, respectively; 3 replicates shown). For
636 graphs shown in (**a**, **c**, **h**, **n**) letters that are different from one another indicate that their means
637 are statistically different ($P \leq 0.05$), and the whiskers represent the standard error of the mean.

638

639 **Figure 5 | Characterization of fusaric acid resistance mutant *ewfR*-7D5::Tn5.** **a**, Genomic
640 organization of the predicted fusaric acid resistance operon showing the position of the Tn5
641 insertion and putative LysR binding site within the promoter (P). **b-c**, The inhibitory effect of
642 fusaric acid embedded within agar on the growth of the *ewfR*⁻ mutant compared to wild type M6.
643 **d**, Quantitative real time PCR gene expression of two protein-coding genes required for the
644 formation of the fusaric acid efflux pump (*ewfD* and *ewfE*) in wild type M6 (+) and the mutant (-
645) (*ewfR*⁻). **e**, Quantification of *ewfR*⁻ mutant strain (M) motility compared to wild type M6 (W),
646 with representative pictures (inset) of motility assays on semisolid agar plates. **f-g**, Light
647 microscopy image showing decreased swarming and colony formation of (**f**) the *ewfR*⁻ mutant

648 strain around Fg hyphae stained with lactophenol blue, compared to (g) wild type M6. h,
649 Electron microscopy image of the *ewfR*⁻ mutant strain. i, Confocal microscopy image showing
650 the attachment pattern of the GFP-tagged *ewfR*⁻ mutant strain (green) to Fg hyphae stained with
651 calcofluor stain, compared to wild type M6 (inset). j, Confocal microscopy image showing a
652 proteinaceous biofilm matrix stained with Ruby film tracer (red) associated with GFP-tagged
653 *ewfR*⁻ mutant strain compared to wild type M6 (inset). k, Spectrophotometric quantification of
654 biofilm formation associated with wild type M6 compared to the *ewfR*⁻ mutant strain, with
655 representative biofilm assay well pictures (left and right, respectively; 3 replicates shown). qRT-
656 PCR analysis of: (l) wild type *ewfR* expression in a wild type M6 background, (m) wild type
657 *ewpR* in an *ewfR*⁻ mutant background, and (n) wild type *ewpR* in a wild type M6 background.
658 For graphs shown in (d, e, k, l- n) letters that are different from one another indicate that their
659 means are statistically different ($P \leq 0.05$; in the case of l-n, within a time point), and the whiskers
660 represent the standard error of the mean.

661

662 **Figure 6 | Characterization of di-guanylate cyclase mutant *ewgS-10A8::Tn5*.** a, Illustration
663 of the enzymatic conversion of 2 guanosine phosphate to c-di-GMP catalyzed by di-guanylate
664 cyclase. b, Complementation of the putative *ewgS*⁻ mutant with respect to inhibition of *F.*
665 *graminearum* (Fg) by addition of c-di-GMP (0.01 and 0.02 mg/ml), compared to wild type strain
666 M6. c, qRT-PCR analysis of wild type *ewgS* expression in a wild type M6 background. d,
667 Quantification of *ewgS*⁻ mutant strain (M) motility compared to wild type M6 (W), with
668 representative pictures (inset) of motility assays on semisolid agar plates. e-f, Light microscopy
669 image showing decrease in swarming and colony formation of (e) *ewgS*⁻ mutant strain around Fg
670 hyphae stained with lactophenol blue, compared to (f) wild type M6. g, Electron microscopy

671 image of *ewgS*⁻ mutant strain. **h**, Confocal microscopy image showing attachment pattern of
672 GFP-tagged *ewgS*⁻ mutant strain (green) to Fg hyphae stained with calcofluor stain, compared to
673 wild type M6 (inset). **i**, Confocal microscopy image showing loss of proteinaceous biofilm
674 matrix stained with Ruby film tracer (red) associated with GFP-tagged *ewgS*⁻ mutant strain
675 compared to wild type M6 (inset). **j**, Spectrophotometric quantification of biofilm formation
676 associated with wild type M6 compared to the *ewgS*⁻ mutant strain, with representative biofilm
677 assay well pictures (left and right, respectively; 3 replicates shown). For graphs shown in (**c**, **d**, **j**)
678 letters that are different from one another indicate that their means are statistically different
679 ($P \leq 0.05$), and the whiskers represent the standard error of the mean.

680

681 **Figure 7 | Characterization of Colicin V Mutant *ewvC*-4B9::Tn5.** **a**, Dual culture agar
682 diffusion assay showing loss of antagonism against the colicin V sensitive *E coli* strain
683 (MC4100) by the *ewvC* mutant compared to wild type M6. **b**, qRT-PCR analysis of wild type
684 *ewvC* expression in a wild type M6 background. **c**, Quantification of *ewvC* mutant strain (M)
685 motility compared to wild type M6 (W), with representative pictures (inset) of motility assays on
686 semisolid agar plates. **d-e**, Light microscopy image showing decrease in swarming and colony
687 formation of (**d**) the *ewvC* mutant strain around Fg hyphae stained with lactophenol blue,
688 compared to (**e**) wild type M6. **f**, Electron microscopy image of the *ewvC* mutant strain. **g**,
689 Confocal microscopy image showing the attachment pattern of the GFP-tagged *ewvC* mutant
690 strain (green) to Fg hyphae stained with calcofluor stain, compared to wild type M6 (inset). **h**,
691 Confocal microscopy image showing the proteinaceous biofilm matrix stained with Ruby film
692 tracer (red) associated with the GFP-tagged *ewvC* mutant strain compared to wild type M6
693 (inset). **i**, Spectrophotometric quantification of biofilm formation associated with wild type M6

694 compared to the *ewvC* mutant strain, with representative biofilm assay well pictures (left and
695 right, respectively; 3 replicates shown). For graphs shown in **(b, c, i)** letters that are different
696 from one another indicate that their means are statistically different ($P \leq 0.05$), and the whiskers
697 represent the standard error of the mean.

698

699 **Supplementary Data**

700 **Supplementary Table 1 | Taxonomic classification of finger millet bacterial endophytes**

701 **based on 16S rDNA sequences and BLAST Analysis.**

702

703 **Supplementary Table 2 | Effect of endophyte strain M6 isolated from finger millet on the**

704 **growth of diverse fungal pathogens *in vitro*.**

705

706 **Supplementary Table 3 | Suppression of *F. graminearum* disease symptoms in maize and**

707 **wheat by endophyte M6 in replicated greenhouse trials.**

708

709 **Supplementary Table 4 | Reduction of DON mycotoxin accumulation during prolonged**

710 **seed storage following treatment with endophyte M6.**

711

712 **Supplementary Table 5 | Complete list of strain M6 Tn5 insertion mutants showing loss of**
713 **antifungal activity against *F. graminearum* in vitro.**

714

715 **Supplementary Table 6 | M6 wild type nucleotide coding sequences²⁶ corresponding to Tn5**
716 **insertion mutants that showed loss of antifungal activity against *F. graminearum* in vitro.**

717

718 **Supplementary Table 7 | Gene-specific primers used in quantitative real-time PCR analysis**
719 **(see Supplemental Methods).**

720

721 **Supplementary Figure 1 | 16S rDNA based phylogenetic tree of finger millet endophytes**
722 **M1-M7.**

723

724 **Supplementary Figure 2 | Image of finger millet seedlings previously seed-coated with**
725 **GFP-tagged M6 showing no pathogenic symptoms, consistent with the strain behaving as**
726 **an endophyte.**

727

728 **Supplementary Figure 3 | Suppression of *F. graminearum* (Fg) by M6 and its effect on**
729 **grain yield in greenhouse trials. a-b, Effect of endophyte M6 on grain yield per plant in two**
730 **greenhouse trials for (a) maize and (b) wheat. c, Effect of treatment with endophyte M6 on Fg**
731 **disease symptoms in maize ears when the endophyte was applied as a seed coat or foliar spray**

732 compared to a *Fusarium* only control treatment. Letters that are different from one another
733 within a trial indicate that their means are statistically different ($P \leq 0.05$). The whiskers indicate
734 the range of data.

735

736 **Supplementary Figure 4 | Assay for production of indole-3-acetic acid (IAA, auxin) by wild**
737 **type strain M6.** Production of indole-3-acetic acid (IAA) *in vitro* by wild type strain M6
738 compared to a positive control (bacterial endophyte strain E10)¹⁰⁷ using the Salkowski reagent
739 colorimetric assay.

740

741 **Supplementary Figure 5 | Tn5 mutagenesis-mediated discovery, validation and**
742 **complementation of genes required for the anti-*Fusarium* activity of strain M6.** **a**, Loss of
743 anti-*F. graminearum* activity associated with each Tn5 insertion mutant using the *in vitro* dual
744 culture diffusion assay, along with a representative image (inset) of the mutant screen. **b-c**, *In*
745 *planta* validation of loss of anti-fungal activity of M6 mutant strains based on quantification of
746 *F. graminearum* disease symptoms on maize ears, in **(b)** greenhouse trial 1, and **(c)** greenhouse
747 trial 2. Only mutant strains that completely lost anti-fungal activity *in vitro* were selected for *in*
748 *planta* validation. The whiskers indicate the range of data points. Letters that are different from
749 one another indicate that their means are statistically different ($P \leq 0.05$). **d**, Genetic
750 complementation of Tn5 mutants with the predicted, corresponding wild type coding sequences.
751 Shown are representative images.

752

753 **Supplementary Figure 6 | Model to illustrate the interaction between strain M6, the host**
754 **plant and *F. graminearum* pathogen.** Following pathogen sensing, M6 swarm towards
755 *Fusarium* hyphae and induces local hair growth, perhaps mediated by M6-IAA production. M6
756 then forms microcolony stacks between the elongated and bent root hairs resulting root hair-
757 endophyte stack (RHESt) formation, likely mediated by biofilms. The RHESt formation
758 prevents entry and/or traps *F. graminearum* for subsequent killing. M6 killing requires diverse
759 antimicrobial compounds including phenazines. *Fusarium* will produce fusaric acid which
760 interferes with phenazine biosynthesis. However, M6 has a specialized fusaric acid-resistance
761 pump system which is predicted to pump the mycotoxin outside the endophyte cell.

762

763 **Supplementary Figure 7 | Assays for production of butanediol and chitinase by strain M6.**
764 **a,** Entire GC chromatogram showing an arrow pointing to a peak with RT 11.13 with a
765 molecular weight and fragmentation pattern (inset) that matches 2, 3 butanediol when searched
766 against the NIST 2008 database. **b,** Quantification of chitinase production by an M6 mutant
767 strain carrying a Tn5 insertion in a chitinase encoding gene (*ewc-3H2::Tn5*) compared to wild
768 type M6 (see Supplementary Table 7).

769

770 **Conflict of Interest Statement**

771 The authors declare that they have no competing financial interests.

772

773 **Author Contributions**

774 WKM designed and conducted all experiments, analyzed all data and wrote the manuscript. CS
775 assisted in the greenhouse trials. VLR performed the DON quantification experiments. CE and
776 JE sequenced the M6 genome and provided gene annotations. MNR helped to design the
777 experiments and edited the manuscript. All authors read and approved the manuscript.

778

779 **Acknowledgements**

780 We are very thankful to Dr. Michaela Streuder (Department of Molecular and Cellular Biology,
781 University of Guelph) for assistance in confocal microscopy experiments and for her insightful
782 comments. We thank Prof. A. Schaafsma and Dr. Ljiljana Tamburic-Ilincic (Ridgetown College,
783 University of Guelph, Canada) for kindly providing hybrid maize and wheat seeds, respectively.
784 We thank Marina Atalla for assistance in disease scoring. WKM was supported by generous
785 scholarships from the Government of Egypt and the University of Guelph (International
786 Graduate Student Scholarships, 2012, 2014). This research was supported by grants to MNR by
787 the Ontario Ministry of Agriculture, Food and Rural Affairs (OMAFRA), Grain Farmers of
788 Ontario (GFO), Natural Sciences and Engineering Research Council of Canada (NSERC) and
789 the CIFSRF program funded by the International Development Research Centre (IDRC, Ottawa)
790 and Canadian Department of Global Affairs.

791

792 **References**

- 793 1 Goron, T. L. & Raizada, M. N. Genetic diversity and genomic resources available for the small
794 millet crops to accelerate a New Green Revolution. *Front. Plant Sci.* **6**, 157 (2015).
795
796 2 Thilakarathna, M. S. & Raizada, M. N. A review of nutrient management studies involving finger
797 millet in the semi-arid tropics of Asia and Africa. *Agronomy* **5**, 262-290 (2015).

- 798
799 3 Hilu, K. W. & de Wet, J. M. J. Domestication of *Eleusine coracana*. *Econ. Bot.* **30**, 199-208 (1976).
800
801 4 Mousa, W. K. *et al.* An endophytic fungus isolated from finger millet (*Eleusine coracana*) produces
802 anti-fungal natural products. *Front. Microbiol.* **6**, 1157(2015).
803
804 5 Sundaramari, P. V. a. M. Rationality and adoption of indigenous cultivation practices of finger millet
805 (*Eleusine coracana* (L.) Gaertn.) by the tribal farmers of Tamil Nadu. *Intl. J. Manag. Social Sci.* **02**,
806 970-977 (2015).
807
808 6 Sutton, J. C. Epidemiology of wheat head blight and maize ear rot caused by *Fusarium*
809 *graminearum*. *Can. J. Plant Pathol.* **4**, 195-209 (1982).
810
811 7 Mousa, W. K., Shearer, C., Limay-Rios, V., Zhou, T. & Raizada, M. N. Bacterial endophytes from
812 wild maize suppress *Fusarium graminearum* in modern maize and inhibit mycotoxin accumulation.
813 *Front. Plant Sci.* **6**, 805 (2015).
814
815 8 Munimbazi, C. & Bullerman, L. B. Molds and mycotoxins in foods from Burundi. *J. Food Prot.* **59**,
816 869-875 (1996).
817
818 9 Chandrashekar, A. & Satyanarayana, K. Disease and pest resistance in grains of sorghum and
819 millets. *J. Cereal Sci.* **44**, 287-304 (2006).
820
821 10 Siwela, M., Taylor, J., de Milliano, W. A. & Duodu, K. G. Influence of phenolics in finger millet on
822 grain and malt fungal load, and malt quality. *Food Chem.* **121**, 443-449 (2010).
823
824 11 Wilson, D. Endophyte: the evolution of a term, and clarification of its use and definition. *Oikos* **73**,
825 274-276 (1995).
826
827 12 Johnston-Monje, D. & Raizada, M. N. Conservation and diversity of seed associated endophytes in
828 across boundaries of evolution, ethnography and ecology. *PLoS ONE* **6**, e20396, (2011).
829
830 13 Waller, F. *et al.* The endophytic fungus *Piriformospora indica* reprograms barley to salt-stress
831 tolerance, disease resistance, and higher yield. *Proc. Natl. Acad. Sci. (USA)* **102**, 13386-13391,
832 (2005).
833
834 14 Haas, D. & Defago, G. Biological control of soil-borne pathogens by fluorescent pseudomonads.
835 *Nat. Rev. Microbiol.* **3**, 307-319 (2005).
836
837 15 Mousa, W. K. & Raizada, M. N. The diversity of anti-microbial secondary metabolites produced by
838 fungal endophytes: An interdisciplinary perspective. *Front. Microbiol.* **4**,65 (2013).
839
840 16 Mousa, W. K. & Raizada, M. N. Biodiversity of genes encoding anti-microbial traits within plant
841 associated microbes. *Front. Plant Sci.* **6**, 231(2015).
842
843 17 O'Donnell, K. *et al.* Phylogenetic analyses of RPB1 and RPB2 support a middle Cretaceous origin
844 for a clade comprising all agriculturally and medically important fusaria. *Fungal Genet. Biol.* **52**, 20-
845 31 (2013).
846
847 18 Saleh, A. A., Esele, J., Logrieco, A., Ritieni, A. & Leslie, J. F. *Fusarium verticillioides* from finger
848 millet in Uganda. *Food Addit. Contam.* **29**, 1762-1769 (2012).

- 849
850 19 Pall, B. & Lakhani, J. Seed mycoflora of ragi, *Eleusine coracana* (L.) Gaertn. *Res. Develop. Rep.* **8**,
851 78-79 (1991).
852
853 20 Amata, R. *et al.* An emended description of *Fusarium brevicatenulatum* and *F. pseudoanthophilum*
854 based on isolates recovered from millet in Kenya. *Fungal Divers.* **43**, 11-25 (2010).
855
856 21 Penugonda, S., Girisham, S. & Reddy, S. Elaboration of mycotoxins by seed-borne fungi of finger
857 millet (*Eleusine coracana* L.). *Intl. J. Biotech. Mol. Biol. Res.* **1**, 62-64 (2010).
858
859 22 Ramana, M. V., Nayaka, S. C., Balakrishna, K., Murali, H. & Batra, H. A novel PCR–DNA probe
860 for the detection of fumonisin-producing *Fusarium* species from major food crops grown in southern
861 India. *Mycology* **3**, 167-174 (2012).
862
863 23 Adipala, E. Seed-borne fungi of finger millet. *E. Afr. Agricult. Forest. J.* **57**, 173-176 (1992).
864
865 24 Dereeper, A. *et al.* Phylogeny. fr: robust phylogenetic analysis for the non-specialist. *Nucleic acids*
866 *Res.* **36**, 465-469 (2008).
867
868 25 Dereeper, A., Audic, S., Claverie, J.-M. & Blanc, G. BLAST-explorer helps you building datasets for
869 phylogenetic analysis. *BMC Evol. Biol.* **10**, 8 (2010).
870
871 26 Ettinger, C. L., Mousa, W. M., Raizada, M. N. & Eisen, J. A. Draft Genome Sequence of
872 *Enterobacter* sp. Strain UCD-UG_FMILLET (Phylum Proteobacteria). *Genome Announc.* **3**, e0146-
873 14 (2015).
874
875 27 Chongo, G. *et al.* Reaction of seedling roots of 14 crop species to *Fusarium graminearum* from
876 wheat heads. *Can. J. Plant Pathol.* **23**, 132-137 (2001).
877
878 28 Pitts, R. J., Cernac, A. & Estelle, M. Auxin and ethylene promote root hair elongation in
879 *Arabidopsis*. *Plant J.* **16**, 553-560 (1998).
880
881 29 Parsons, J. F. *et al.* Structure and function of the phenazine biosynthesis protein PhzF from
882 *Pseudomonas fluorescens* 2-79. *Biochemistry* **43**, 12427-12435 (2004).
883
884 30 Lu, J. *et al.* LysR family transcriptional regulator PqsR as repressor of pyoluteorin biosynthesis and
885 activator of phenazine-1-carboxylic acid biosynthesis in *Pseudomonas* sp. M18. *J. Biotechnol.* **143**,
886 1-9 (2009).
887
888 31 Goethals, K., Van Montagu, M. & Holsters, M. Conserved motifs in a divergent nod box of
889 *Azorhizobium caulinodans* ORS571 reveal a common structure in promoters regulated by LysR-type
890 proteins. *Proc. Natl. Acad. Sci. (USA)* **89**, 1646-1650 (1992).
891
892 32 Wang, Y., Luo, Q., Zhang, X. & Wang, W. Isolation and purification of a modified phenazine,
893 griseoluteic acid, produced by *Streptomyces griseoluteus* P510. *Res. Microbiol.* **162**, 311-319,
894 (2011).
895
896 33 Nakamura, S., Wang, E. L., Murase, M., Maeda, K. & Umezawa, H. Structure of griseolutein A. *J.*
897 *Antibiot.* **12**, 55-58 (1959).
898

- 899 34 Giddens, S. R., Feng, Y. & Mahanty, H. K. Characterization of a novel phenazine antibiotic gene
900 cluster in *Erwinia herbicola* Eh1087. *Mol. Microbiol.* **45**, 769-783 (2002).
901
- 902 35 Kitahara, M. *et al.* Saphenamycin, a novel antibiotic from a strain of *Streptomyces*. *J. Antibiot.* **35**,
903 1412-1414 (1982).
904
- 905 36 Toyoda, H., Katsuragi, K., Tamai, T. & Ouchi, S. DNA Sequence of genes for detoxification of
906 fusaric acid, a wilt-inducing agent produced by *Fusarium* species. *J. Phytopathol.* **133**, 265-277
907 (1991).
908
- 909 37 Utsumi, R. *et al.* Molecular cloning and characterization of the fusaric acid-resistance gene from
910 *Pseudomonas cepacia*. *Agri. Biol. Chem.* **55**, 1913-1918 (1991).
911
- 912 38 Marre, M., Vergani, P. & Albergoni, F. Relationship between fusaric acid uptake and its binding to
913 cell structures by leaves of *Egeria densa* and its toxic effects on membrane permeability and
914 respiration. *Physiol. Mol. Plant Pathol.* **42**, 141-157 (1993).
915
- 916 39 Bacon, C., Hinton, D. & Hinton, A. Growth-inhibiting effects of concentrations of fusaric acid on the
917 growth of *Bacillus mojavensis* and other biocontrol *Bacillus* species. *J. App. Microbiol.* **100**, 185-194
918 (2006).
919
- 920 40 Borges-Walmsley, M., McKeegan, K. & Walmsley, A. Structure and function of efflux pumps that
921 confer resistance to drugs. *Biochem. J.* **376**, 313-338 (2003).
922
- 923 41 Hu, R.-M., Liao, S.-T., Huang, C.-C., Huang, Y.-W. & Yang, T.-C. An inducible fusaric acid
924 tripartite efflux pump contributes to the fusaric acid resistance in *Stenotrophomonas maltophilia*.
925 *PLoS ONE* **7**, e51053 (2012).
926
- 927 42 van Rij, E. T., Girard, G., Lugtenberg, B. J. & Bloemberg, G. V. Influence of fusaric acid on
928 phenazine-1-carboxamide synthesis and gene expression of *Pseudomonas chlororaphis* strain
929 PCL1391. *Microbiology* **151**, 2805-2814 (2005).
930
- 931 43 Römling, U., Galperin, M. Y. & Gomelsky, M. Cyclic di-GMP: the first 25 years of a universal
932 bacterial second messenger. *Microbiol. Mol. Biol. Rev.* **77**, 1-52 (2013).
933
- 934 44 Fath, M., Mahanty, H. & Kolter, R. Characterization of a purF operon mutation which affects colicin
935 V production. *J. Bacteriol.* **171**, 3158-3161 (1989).
936
- 937 45 Fath, M. J., Zhang, L. H., Rush, J. & Kolter, R. Purification and characterization of colicin V from
938 *Escherichia coli* culture supernatants. *Biochemistry* **33**, 6911-6917 (1994).
939
- 940 46 Soliman, S. S. *et al.* An endophyte constructs fungicide-containing extracellular barriers for its host
941 plant. *Curr. Biol.* **25**, 2570-2576 (2015).
942
- 943 47 Reinhold-Hurek, B., Büniger, W., Burbano, C. S., Sabale, M. & Hurek, T. Roots shaping their
944 microbiome: global hotspots for microbial activity. *Ann. Rev. Phytopathol.* **53**, 403-424 (2015).
945
- 946 48 Compant, S., Clément, C. & Sessitsch, A. Plant growth-promoting bacteria in the rhizo-and
947 endosphere of plants: their role, colonization, mechanisms involved and prospects for utilization. *Soil*
948 *Biol. Biochem.* **42**, 669-678 (2010).
949

- 950 49 Glaeser, S. P. *et al.* Non-pathogenic *Rhizobium radiobacter* F4 deploys plant beneficial activity
951 independent of its host *Piriformospora indica*. *ISME J. in press* (2015).
952
- 953 50 Germaine, K. J., Keogh, E., Ryan, D. & Dowling, D. N. Bacterial endophyte-mediated naphthalene
954 phytoprotection and phytoremediation. *FEMS Microbiol. Lett.* **296**, 226-234 (2009).
955
- 956 51 Marasco, R. *et al.* A drought resistance-promoting microbiome is selected by root system under
957 desert farming. *PLoS ONE* **7**, e48479 (2012).
958
- 959 52 Dandurand, L., Schotzko, D. & Knudsen, G. Spatial patterns of rhizoplane populations of
960 *Pseudomonas fluorescens*. *Appl. Environmen. Microbiol.* **63**, 3211-3217 (1997).
961
- 962 53 Foster, R. The ultrastructure of the rhizoplane and rhizosphere. *Ann. Rev. Phytopathol.* **24**, 211-234
963 (1986).
964
- 965 54 Fukui, R. *et al.* Spatial colonization patterns and interaction of bacteria on inoculated sugar beet
966 seed. *Phytopathology* **84**, 1338-1345 (1994).
967
- 968 55 Rovira, A. A study of the development of the root surface microflora during the initial stages of plant
969 growth. *J. Appl. Bacteriol.* **19**, 72-79 (1956).
970
- 971 56 Rovira, A. & Campbell, R. Scanning electron microscopy of microorganisms on the roots of wheat.
972 *Microb. Ecol.* **1**, 15-23 (1974).
973
- 974 57 Newman, E. & Bowen, H. Patterns of distribution of bacteria on root surfaces. *Soil Biol. Biochem.* **6**,
975 205-209 (1974).
976
- 977 58 Mercado-Blanco, J. & Prieto, P. Bacterial endophytes and root hairs. *Plant Soil* **361**, 301-306 (2012).
978
- 979 59 Danhorn, T. & Fuqua, C. Biofilm formation by plant-associated bacteria. *Annu. Rev. Microbiol.* **61**,
980 401-422 (2007).
981
- 982 60 Lee, R. D.-W. & Cho, H.-T. Auxin, the organizer of the hormonal/environmental signals for root hair
983 growth. *Front. Plant Sci.* **4**, 448 (2013).
984
- 985 61 Patten, C. L. & Glick, B. R. Bacterial biosynthesis of indole-3-acetic acid. *Can. J. Microbiol.* **42**,
986 207-220 (1996).
987
- 988 62 Oldroyd, G. E. Speak, friend, and enter: signalling systems that promote beneficial symbiotic
989 associations in plants. *Nat. Rev. Microbiol.* **11**, 252-263 (2013).
990
- 991 63 Du, X., Li, Y., Zhou, Q. & Xu, Y. Regulation of gene expression in *Pseudomonas aeruginosa* M18
992 by phenazine-1-carboxylic acid. *Appl. Microbiol. Biotechnol.* **99**, 813-825 (2015).
993
- 994 64 Srivastava, D. & Waters, C. M. A tangled web: regulatory connections between quorum sensing and
995 cyclic di-GMP. *J. Bacteriol.* **194**, 4485-4493 (2012).
996
- 997 65 Flemming, H.-C. & Wingender, J. The biofilm matrix. *Nat. Rev. Microbiol.* **8**, 623-633 (2010).
998
- 999 66 An, S.Q. *et al.* Novel cyclic di-GMP effectors of the YajQ protein family control bacterial virulence.
1000 *PLoS Pathog.* **10**, e1004429 (2014).

- 1001
1002 67 Landini, P., Antoniani, D., Burgess, J. G. & Nijland, R. Molecular mechanisms of compounds
1003 affecting bacterial biofilm formation and dispersal. *Appl. Microbiol. Biotechnol.* **86**, 813-823 (2010).
1004
1005 68 Steinberg, N. & Kolodkin-Gal, I. The matrix reloaded: probing the extracellular matrix synchronizes
1006 bacterial communities. *J. Bacteriol.* **197**, 2092–2103 (2015).
1007
1008 69 Cortes-Barco, A., Hsiang, T. & Goodwin, P. Induced systemic resistance against three foliar diseases
1009 of *Agrostis stolonifera* by (2R, 3R)-butanediol or an isoparaffin mixture. *Annal. Appl. Biol.* **157**, 179-
1010 189 (2010).
1011
1012 70 Mavrodi, D. V. *et al.* Recent insights into the diversity, frequency and ecological roles of phenazines
1013 in fluorescent *Pseudomonas* spp. *Environmen. Microbiol.* **15**, 675-686 (2013).
1014
1015 71 Gurusiddaiah, S., Weller, D., Sarkar, A. & Cook, R. Characterization of an antibiotic produced by a
1016 strain of *Pseudomonas fluorescens* inhibitory to *Gaeumannomyces graminis* var. tritici and *Pythium*
1017 spp. *Antimicrob. Agents Chemotherap.* **29**, 488-495 (1986).
1018
1019 72 Anjaiah, V. *et al.* Involvement of phenazines and anthranilate in the antagonism of *Pseudomonas*
1020 *aeruginosa* PNA1 and Tn5 Derivatives toward *Fusarium* spp. and *Pythium* spp. *Mol. Plant-Microb.*
1021 *Interact.* **11**, 847-854 (1998).
1022
1023 73 Bloemberg, G. V. & Lugtenberg, B. J. Phenazines and their role in biocontrol by *Pseudomonas*
1024 bacteria. *New Phytol.* **157**, 503-523 (2003).
1025
1026 74 Hori, M., Nozaki, S., Nagami, K., Asakura, H. & Umezawa, H. Inhibition of DNA synthesis by
1027 griseolutein in *Escherichia coli* through a possible interaction at the cell surface. *Biochimica et*
1028 *Biophysica Acta (BBA)-Nuc. Acids Protein Synth.* **521**, 101-110 (1978).
1029
1030 75 Hassan, H. M. & Fridovich, I. Mechanism of the antibiotic action pyocyanine. *J. Bacteriol.* **141**, 156-
1031 163 (1980).
1032
1033 76 Hassett, D. J., Schweizer, H. P. & Ohman, D. E. *Pseudomonas aeruginosa* sodA and sodB mutants
1034 defective in manganese-and iron-cofactored superoxide dismutase activity demonstrate the
1035 importance of the iron-cofactored form in aerobic metabolism. *J. Bacteriol.* **177**, 6330-6337 (1995).
1036
1037 77 Audenaert, K., Pattery, T., Cornelis, P. & Hofte, M. Induction of systemic resistance to *Botrytis*
1038 *cinerea* in tomato by *Pseudomonas aeruginosa* 7NSK2: role of salicylic acid, pyochelin, and
1039 pyocyanin. *Mol. Plant. Microbe Interact.* **15**, 1147-1156 (2002).
1040
1041 78 Price-Whelan, A., Dietrich, L. E. & Newman, D. K. Rethinking 'secondary' metabolism:
1042 physiological roles for phenazine antibiotics. *Nat. Chem. Biol.* **2**, 71-78 (2006).
1043
1044 79 Wang, Y. & Newman, D. K. Redox reactions of phenazine antibiotics with ferric (hydr) oxides and
1045 molecular oxygen. *Environ. Sci. Technol.* **42**, 2380-2386 (2008).
1046
1047 80 Hernandez, M. & Newman, D. Extracellular electron transfer. *Cell. Mol. Life Sci.* **58**, 1562-1571
1048 (2001).
1049
1050 81 Fu, Y.-C., Zhang, T. & Bishop, P. Determination of effective oxygen diffusivity in biofilms grown in
1051 a completely mixed biodrum reactor. *Water Sci. Technol.* **29**, 455-462 (1994).

- 1052
1053 82 Stewart, P. S. Diffusion in biofilms. *J. Bacteriol.* **185**, 1485-1491 (2003).
1054
1055 83 Whitchurch, C. B., Tolker-Nielsen, T., Ragas, P. C. & Mattick, J. S. Extracellular DNA required for
1056 bacterial biofilm formation. *Science* **295**, 1487-1487 (2002).
1057
1058 84 Petersen, F. C., Tao, L. & Scheie, A. A. DNA binding-uptake system: a link between cell-to-cell
1059 communication and biofilm formation. *J. Bacteriol.* **187**, 4392-4400 (2005).
1060
1061 85 Das, T., Sharma, P. K., Busscher, H. J., van der Mei, H. C. & Krom, B. P. Role of extracellular DNA
1062 in initial bacterial adhesion and surface aggregation. *Appl. Environ. Microbiol.* **76**, 3405-3408
1063 (2010).
1064
1065 86 Das, T., Kutty, S. K., Kumar, N. & Manefield, M. Pyocyanin facilitates extracellular DNA binding to
1066 *Pseudomonas aeruginosa* influencing cell surface properties and aggregation. *PLoS ONE* **8**, e58299
1067 (2013).
1068
1069 87 Das, T. & Manefield, M. Pyocyanin promotes extracellular DNA release in *Pseudomonas*
1070 *aeruginosa*. *PLoS ONE* **7**, e46718. (2012).
1071
1072 88 Das, T. *et al.* Phenazine virulence factor binding to extracellular DNA is important for *Pseudomonas*
1073 *aeruginosa* biofilm formation. *Sci. Rep.* **5**, 8398 (2015).
1074
1075 89 Pierson III, L. S. & Pierson, E. A. Metabolism and function of phenazines in bacteria: impacts on the
1076 behavior of bacteria in the environment and biotechnological processes. *Appl. Microbiol. Biotechnol.*
1077 **86**, 1659-1670 (2010).
1078
1079 90 Gérard, F., Pradel, N. & Wu, L.-F. Bactericidal activity of colicin V is mediated by an inner
1080 membrane protein, SdaC, of *Escherichia coli*. *J. Bacteriol.* **187**, 1945-1950 (2005).
1081
1082 91 Gillor, O. & Ghazaryan, L. Recent advances in bacteriocin application as antimicrobials. *Recent Pat.*
1083 *Anti-infect. Drug Discov.* **2**, 115-122 (2007).
1084
1085 92 Hammami, I., Triki, M. & Rebai, A. Purification and characterization of the novel bacteriocin bac
1086 ih7 with antifungal and antibacterial properties. *J. Plant Pathol.* **93**, 443-454 (2011).
1087
1088 93 Dahiya, N., Tewari, R. & Hoondal, G. S. Biotechnological aspects of chitinolytic enzymes: a review.
1089 *Appl. Microbiol. Biotechnol.* **71**, 773-782 (2005).
1090
1091 94 Dahiya, N., Tewari, R., Tiwari, R. P. & Hoondal, G. S. Production of an antifungal chitinase from
1092 *Enterobacter* sp. NRG4 and its application in protoplast production. *World J. Microbiol. Biotechnol.*
1093 **21**, 1611-1616 (2005).
1094
1095 95 Burkhead, K. D., Slininger, P. J. & Schisler, D. A. Biological control bacterium *Enterobacter*
1096 *cloacae* S11:T:07 (NRRL B-21050) produces the antifungal compound phenylacetic acid in
1097 Sabouraud maltose broth culture. *Soil Biol. Biochem.* **30**, 665-667 (1998).
1098
1099 96 Slininger, P., Burkhead, K. & Schisler, D. Antifungal and sprout regulatory bioactivities of
1100 phenylacetic acid, indole-3-acetic acid, and tyrosol isolated from the potato dry rot suppressive
1101 bacterium *Enterobacter cloacae* S11: T: 07. *J. Ind. Microbiol. Biotechnol.* **31**, 517-524 (2004).
1102

- 1103 97 Schisler, D. A., Slininger, P. J., Kleinkopf, G., Bothast, R. J. & Ostrowski, R. C. Biological control
1104 of *Fusarium* dry rot of potato tubers under commercial storage conditions. *Am. J. Potato Res.* **77**, 29-
1105 40 (2000).
1106
- 1107 98 Herbert, R. B. & Knaggs, A. R. Biosynthesis of the antibiotic obafluorin from p-aminophenylalanine
1108 and glycine (glyoxylate). *J. Chem. Soci. (Perkin Transactions)* **1**, 109-113 (1992).
1109
- 1110 99 Lewis, E. A., Adamek, T. L., Vining, L. C. & White, R. L. Metabolites of a blocked chloramphenicol
1111 producer. *J. Nat. Prod.* **66**, 62-66 (2003).
1112
- 1113 100 He, J., Magarvey, N., Pirae, M. & Vining, L. The gene cluster for chloramphenicol biosynthesis in
1114 *Streptomyces venezuelae* ISP5230 includes novel shikimate pathway homologues and a
1115 monomodular non-ribosomal peptide synthetase gene. *Microbiology* **147**, 2817-2829 (2001).
1116
- 1117 101 Wang, K., Kang, L., Anand, A., Lazarovits, G. & Mysore, K. S. Monitoring *in planta* bacterial
1118 infection at both cellular and whole-plant levels using the green fluorescent protein variant GFPuv.
1119 *New Phytol.* **174**, 212-223 (2007).
1120
- 1121 102 Solovyev, V. & Salamov, A. Automatic annotation of microbial genomes and metagenomic
1122 sequences. in *Metagenomics and its Applications in Agriculture, Biomedicine and Environmental*
1123 *Studies* (ed. Robert, W. Li), 61-78 (Nova Science, 2011).
1124
- 1125 103 de Jong, A., Pietersma, H., Cordes, M., Kuipers, O. P. & Kok, J. PePPER: a webserver for prediction
1126 of prokaryote promoter elements and regulons. *BMC Genom.* **13**, 299 (2012).
1127
- 1128 104 Stepanović, S., Vuković, D., Dakić, I., Savić, B. & Švabić-Vlahović, M. A modified microtiter-plate
1129 test for quantification of staphylococcal biofilm formation. *J. Microbiol. Methods* **40**, 175-179
1130 (2000).
1131
- 1132 105 Bacon, C., Hinton, D. & Hinton, A. Growth-inhibiting effects of concentrations of fusaric acid on the
1133 growth of *Bacillus mojavensis* and other biocontrol *Bacillus* species. *J. Appl. Microbiol.* **100**, 185-
1134 194 (2006).
1135
- 1136 106 Paulus, H. & Gray, E. The biosynthesis of polymyxin B by growing cultures of *Bacillus polymyxa*. *J.*
1137 *Biol. Chem.* **239**, 865-871 (1964).
1138
- 1139 107 Shehata, H. Molecular and physiological mechanisms underlying the antifungal and nutrient
1140 acquisition activities of beneficial microbes. *PhD thesis, University of Guelph, ON Canada.* (2016).

1141

1142

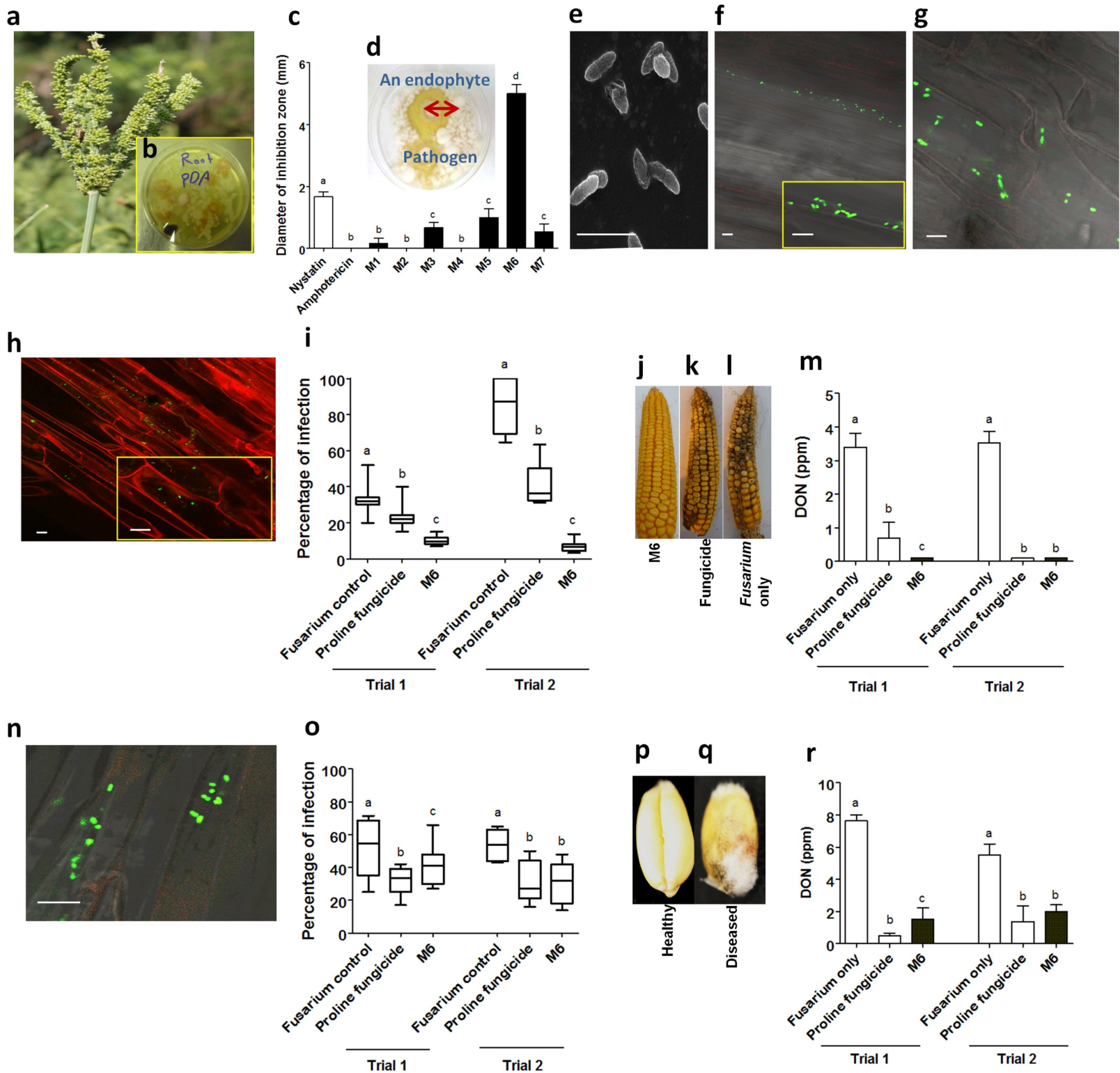
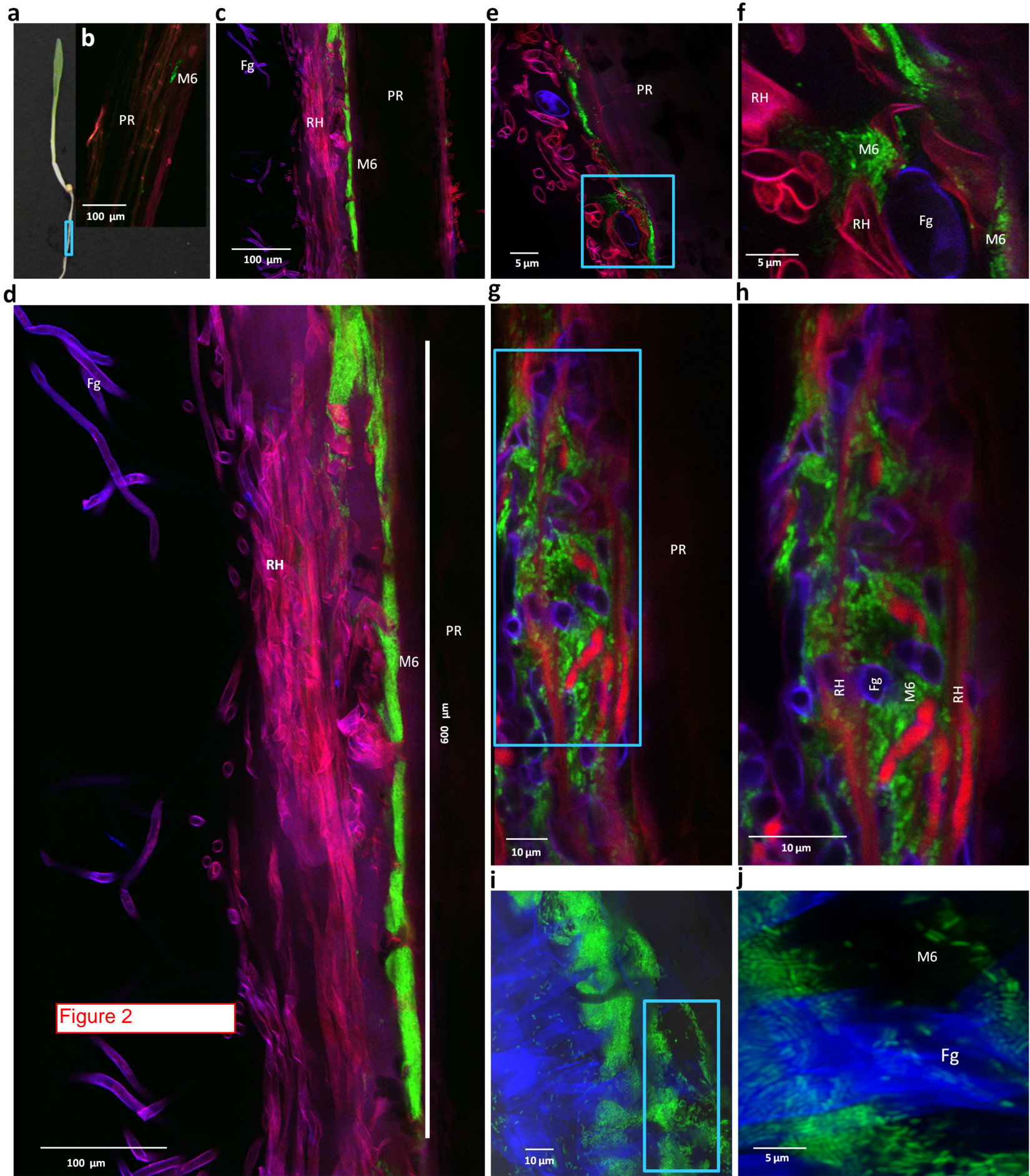


Figure 1



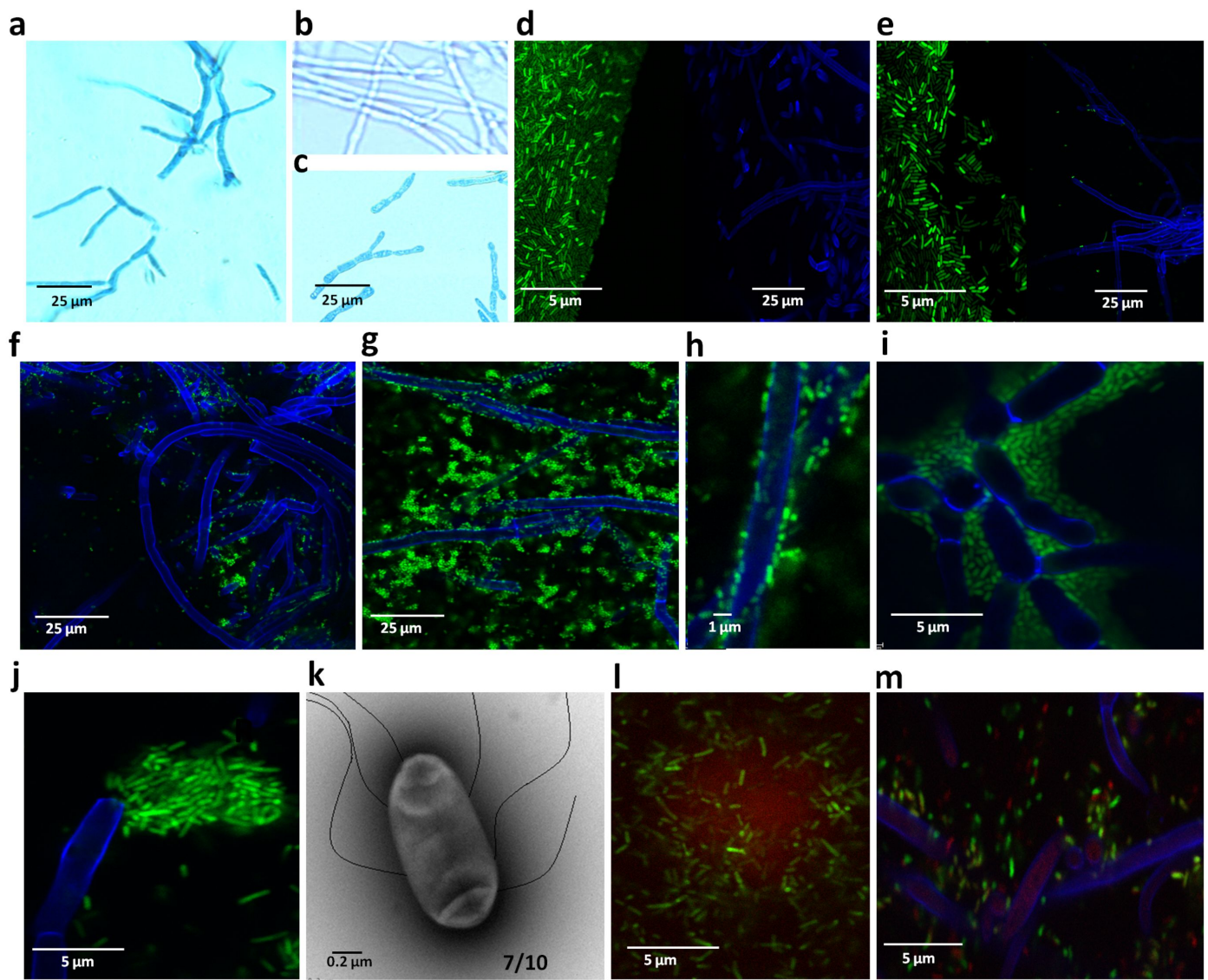


Figure 3

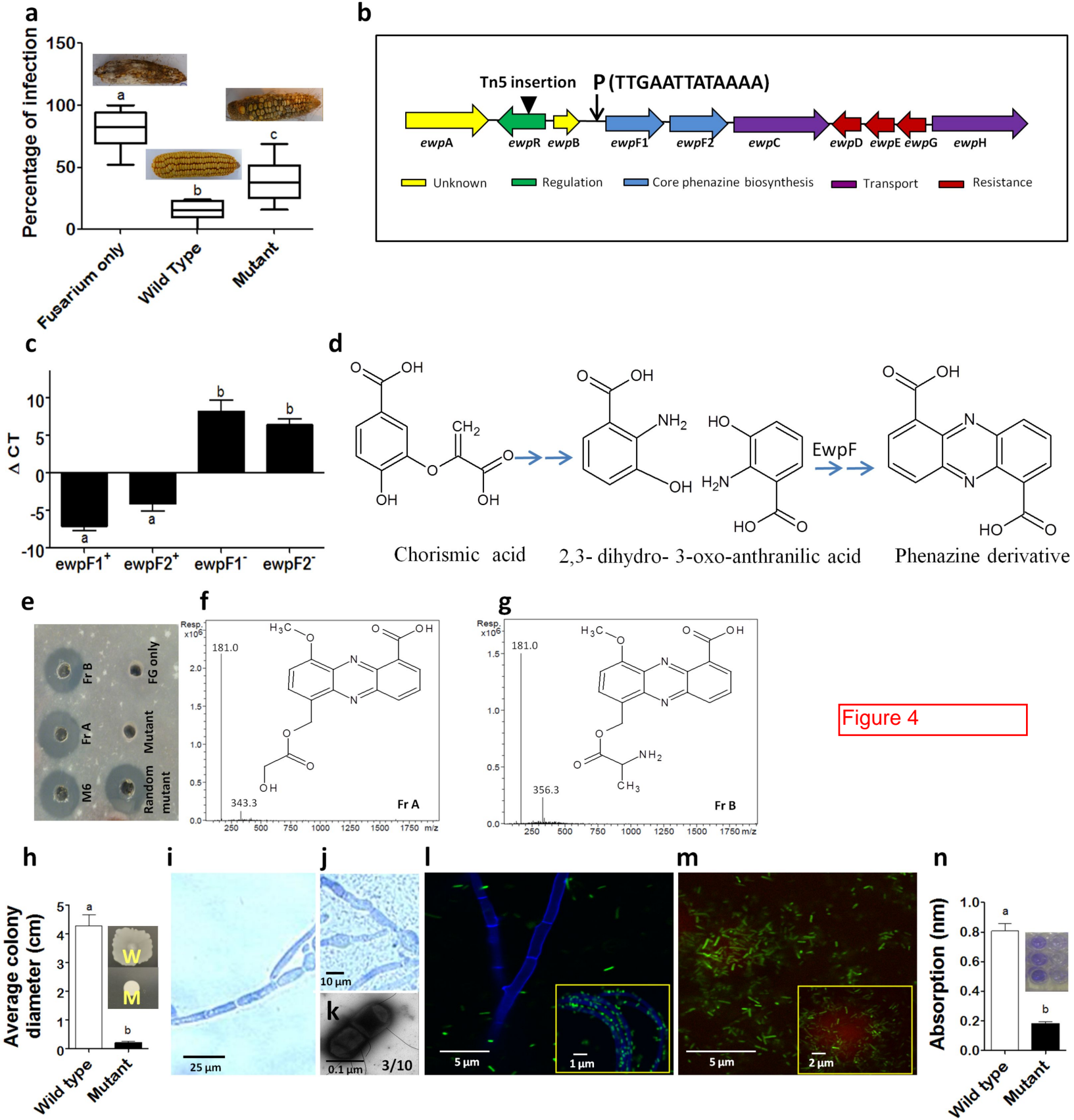
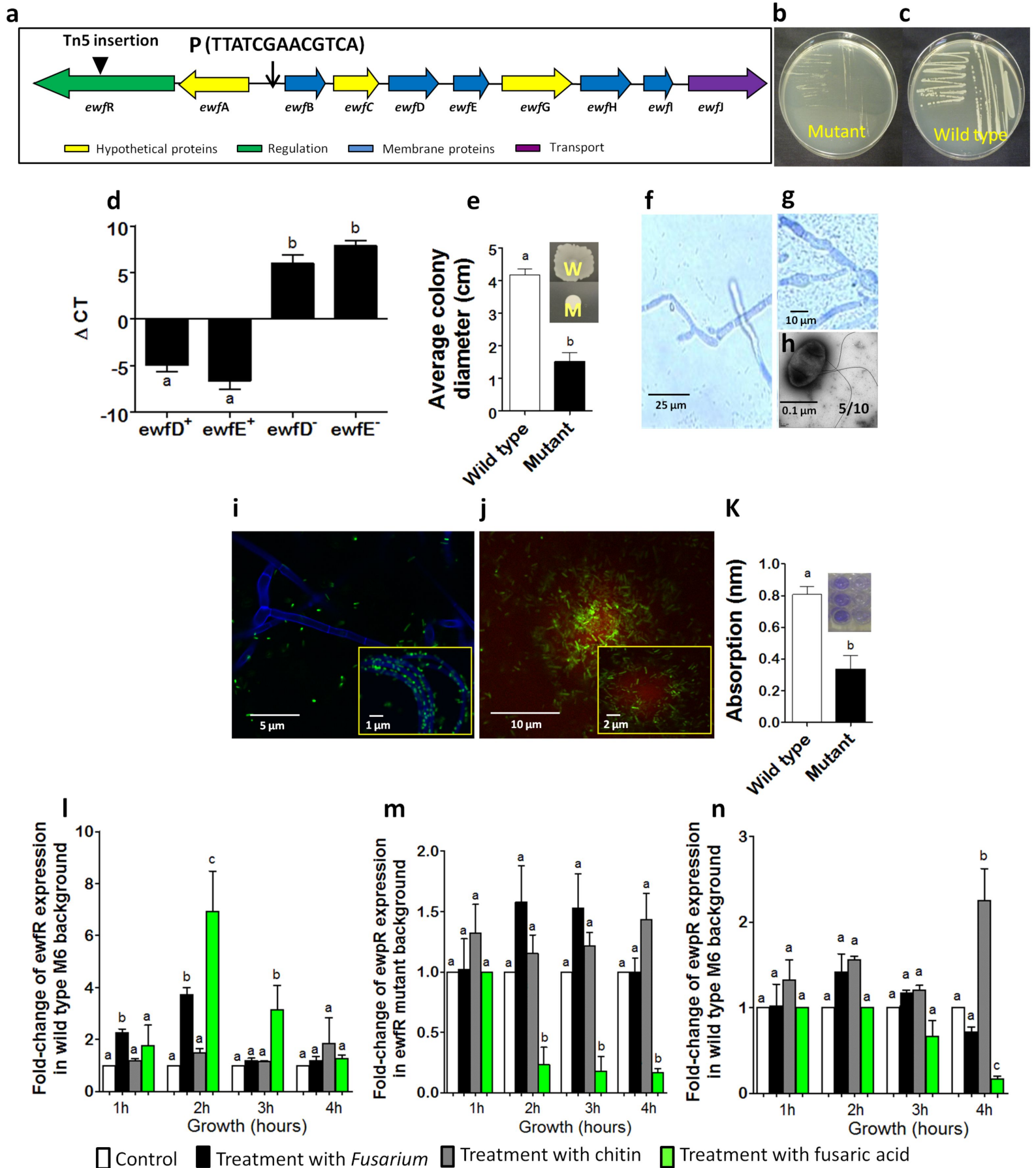


Figure 5



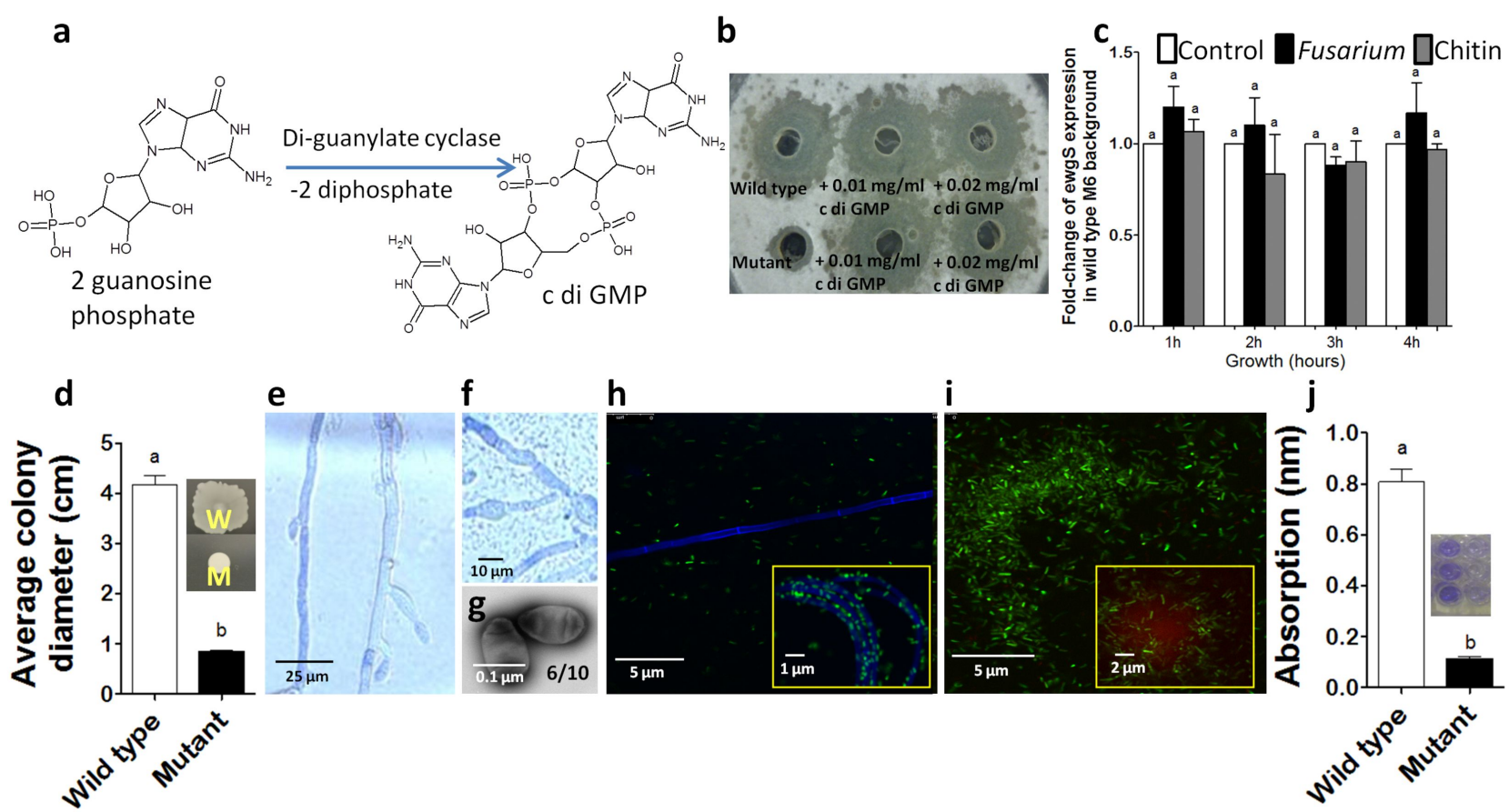


Figure 6

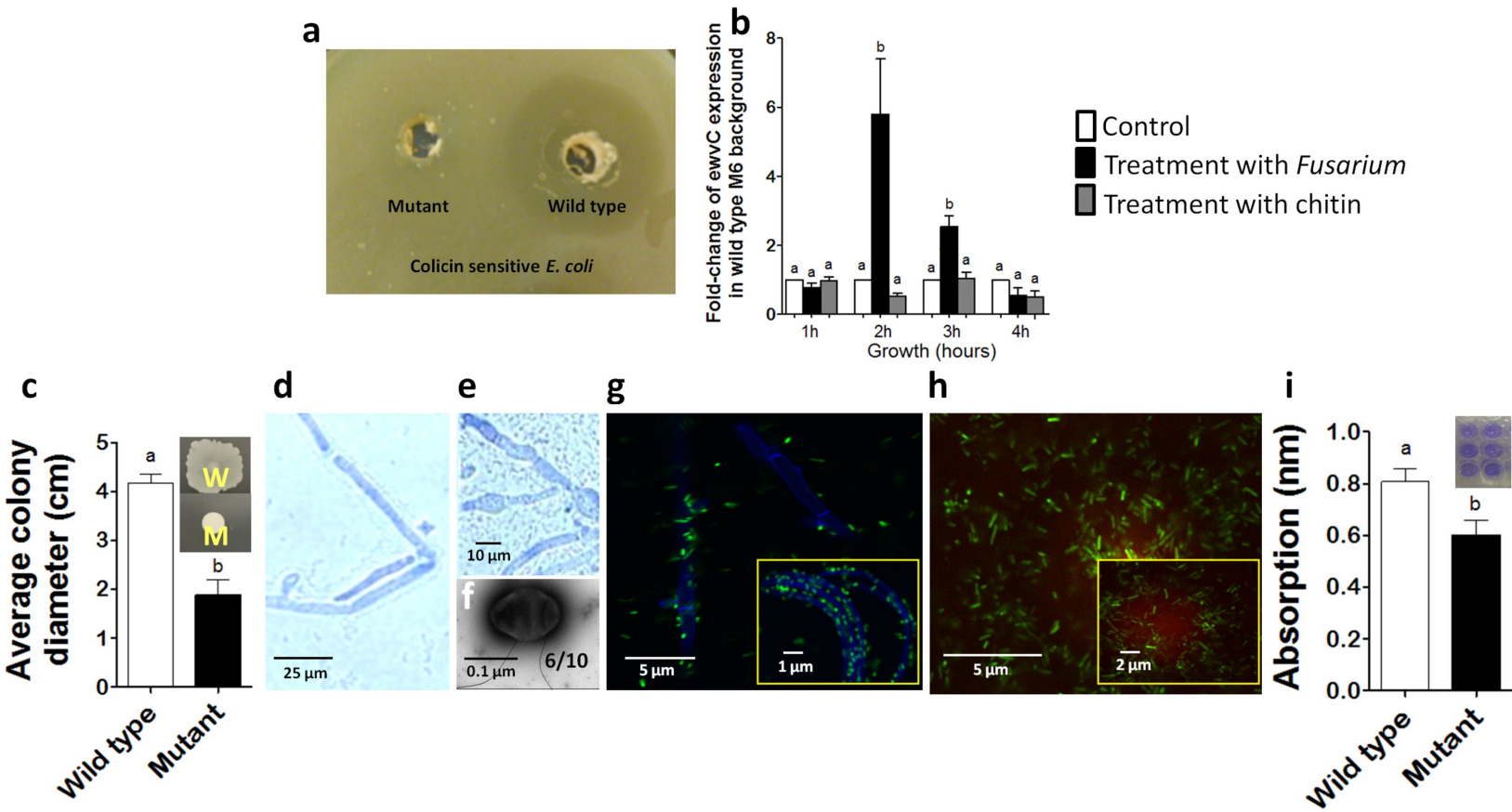


Figure 7

Figure S1

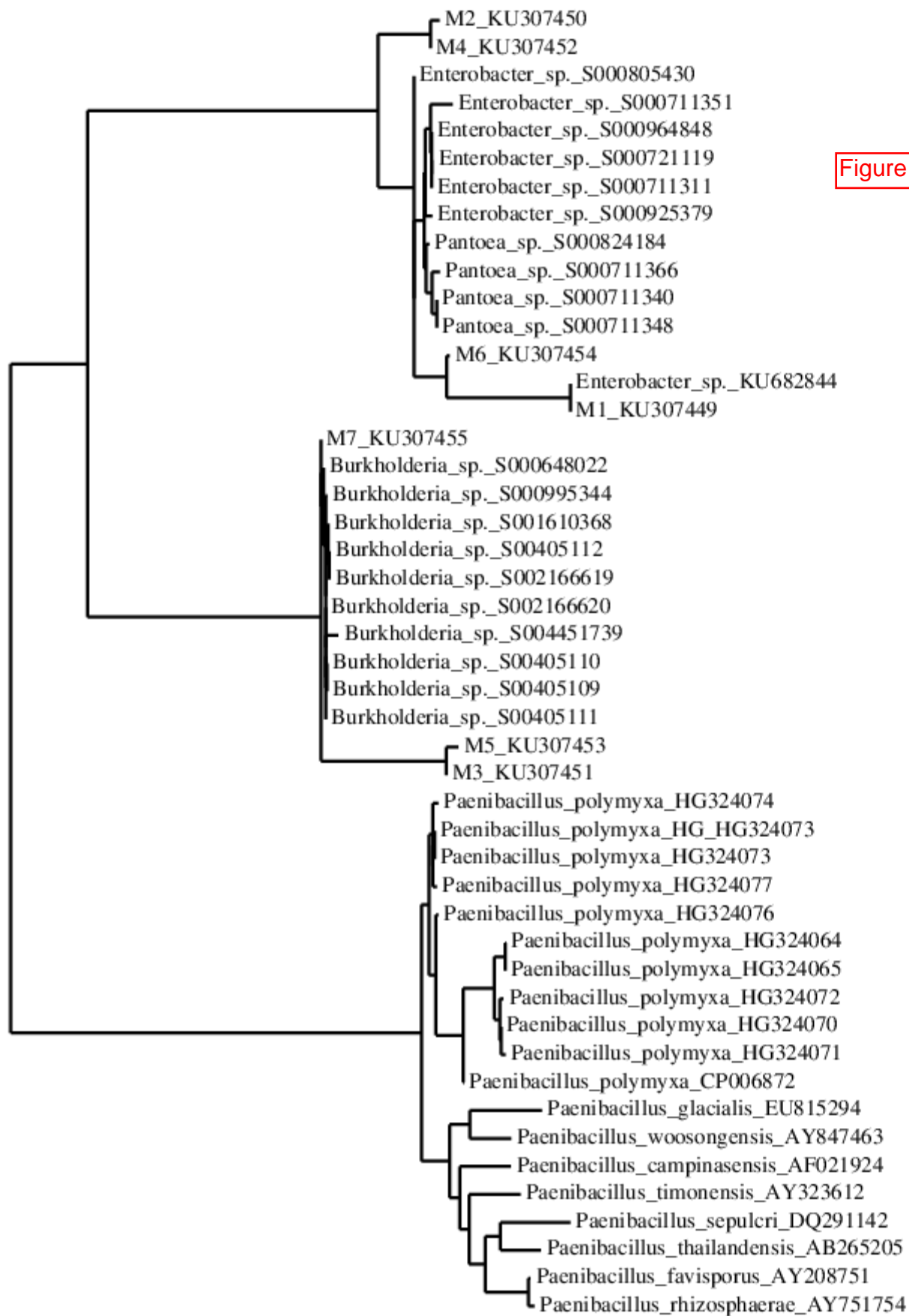


Figure S2



Figure S3

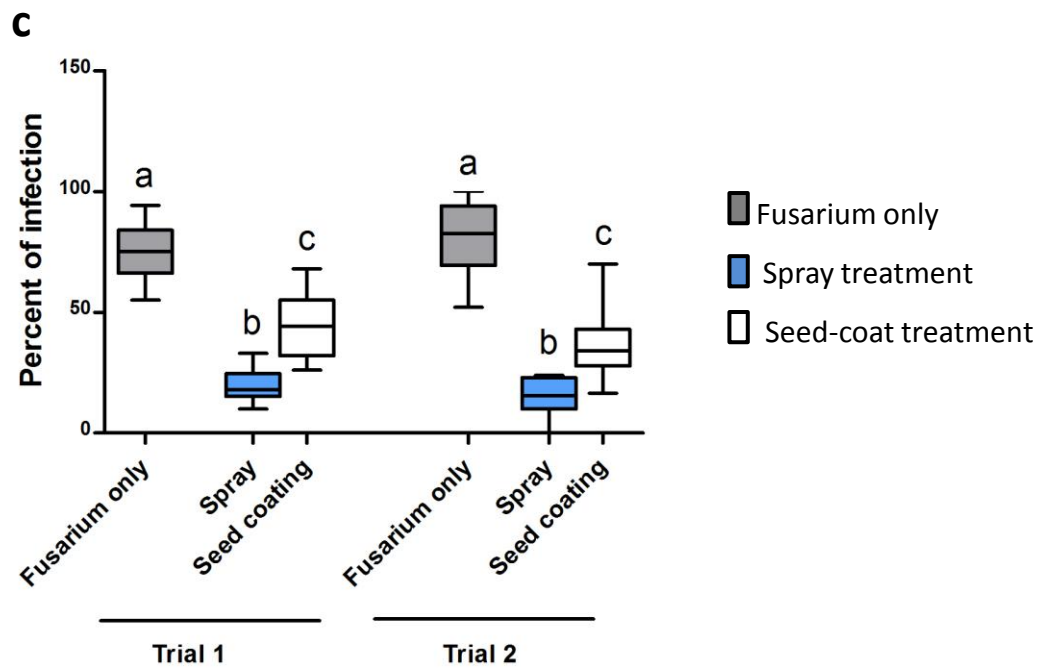
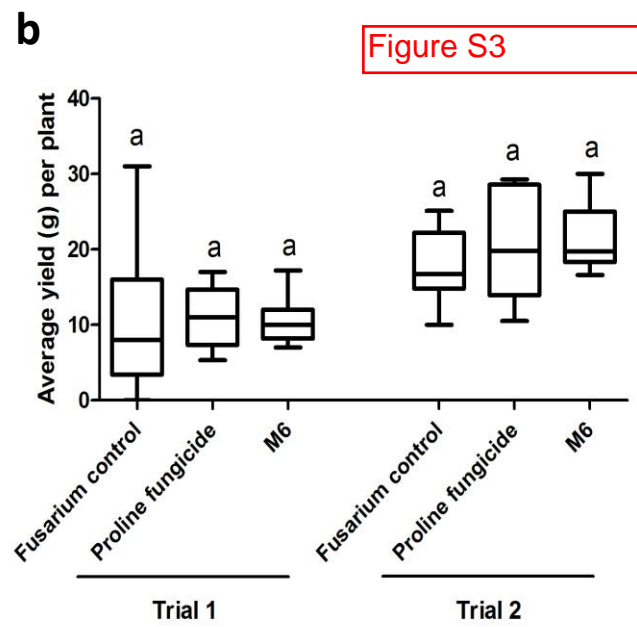
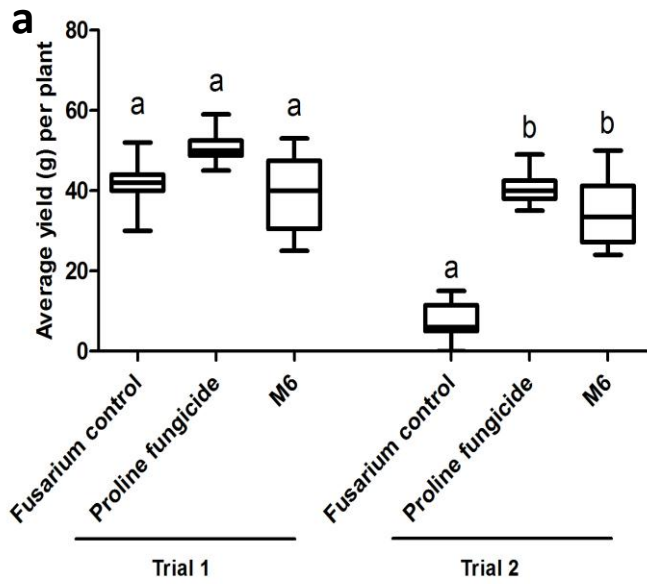
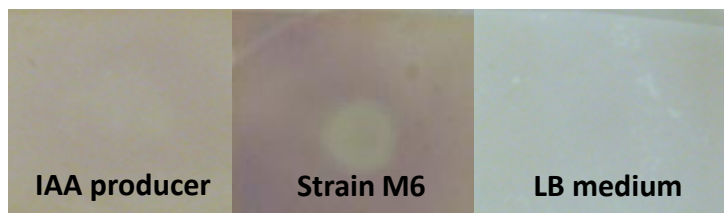


Figure S4



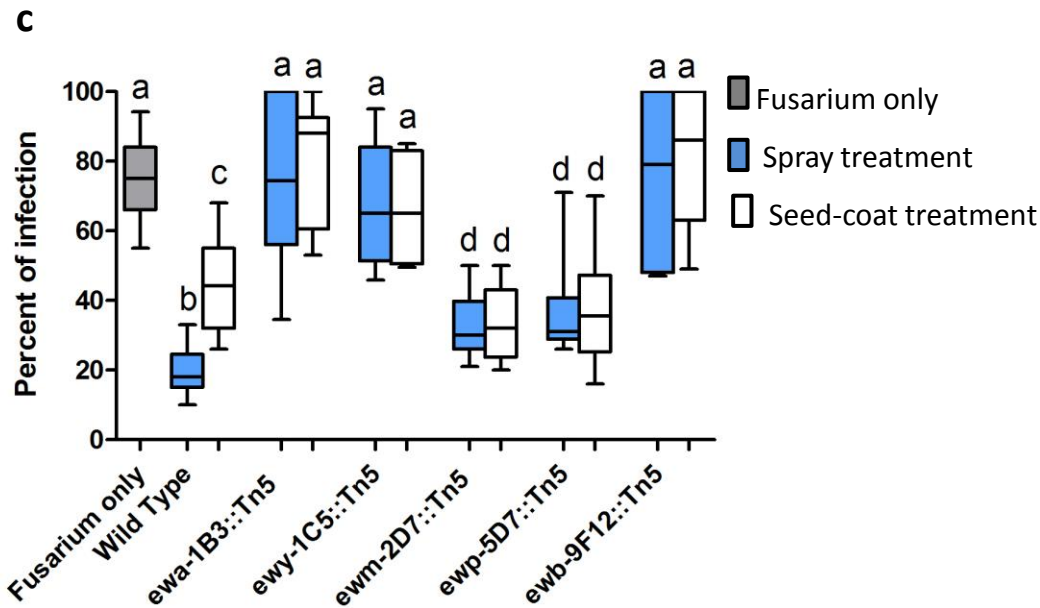
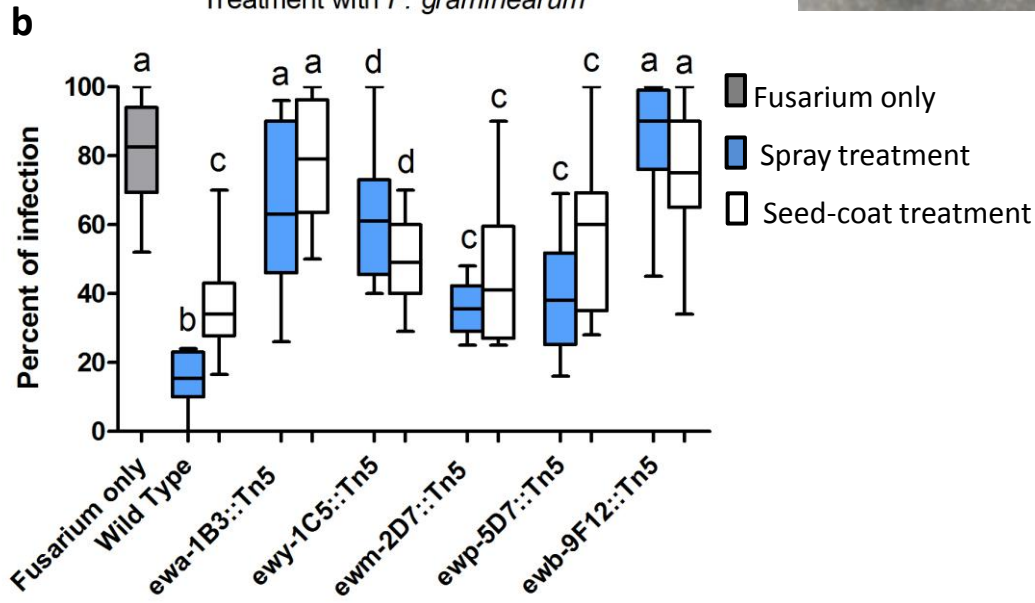
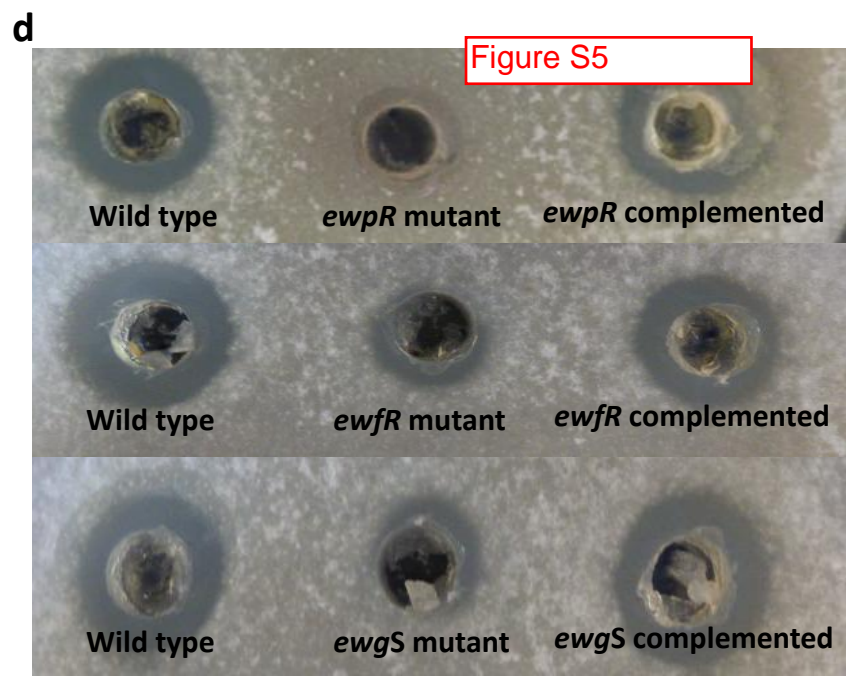
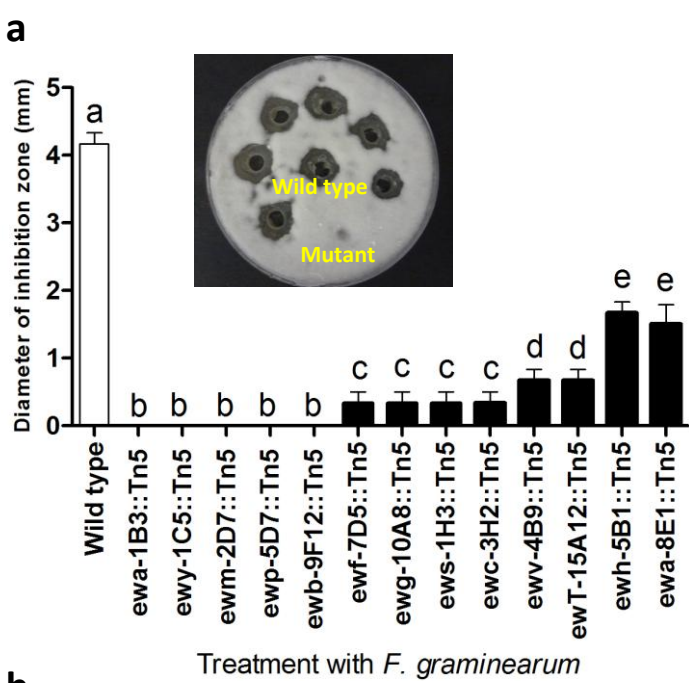


Figure S6

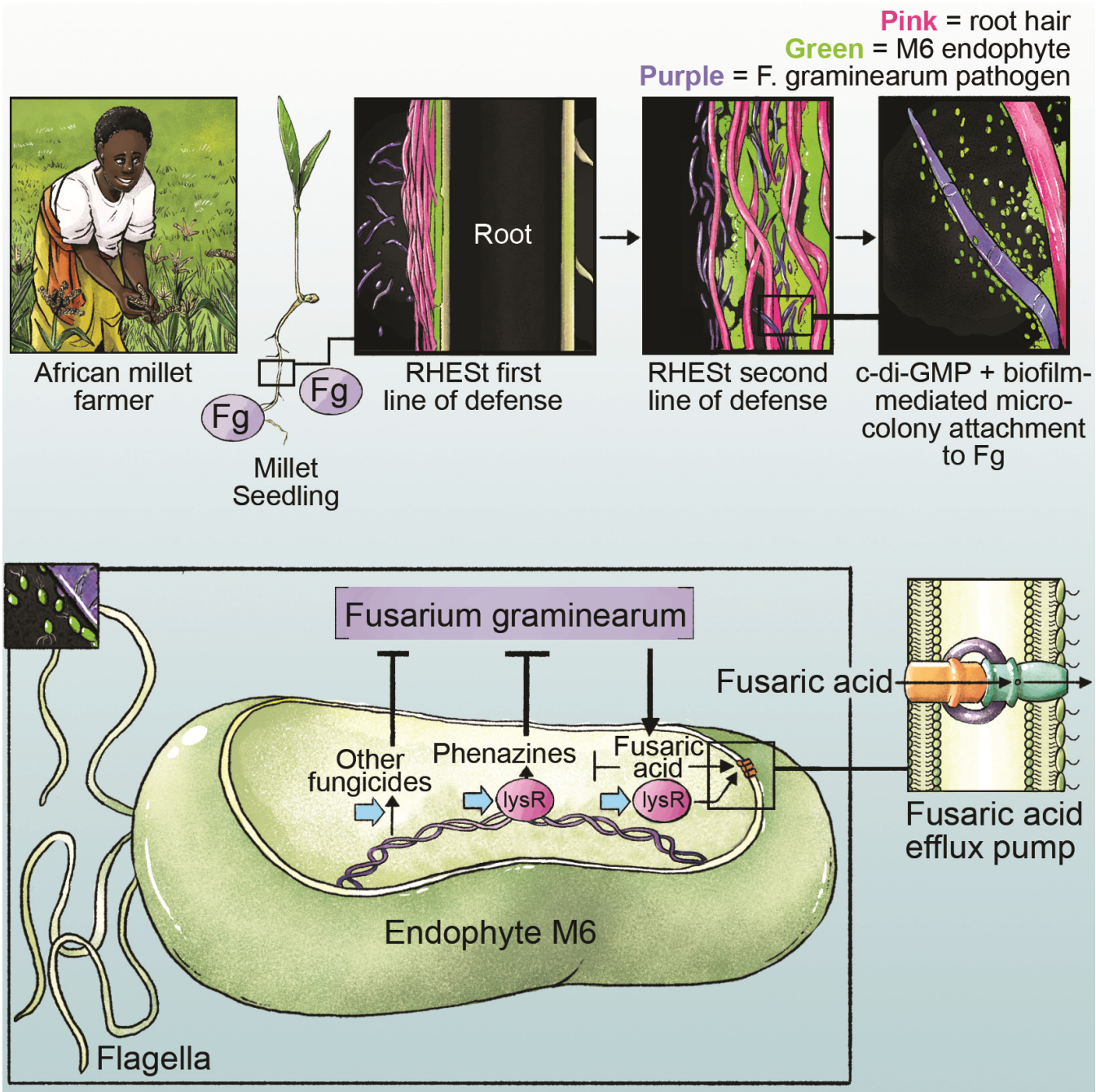
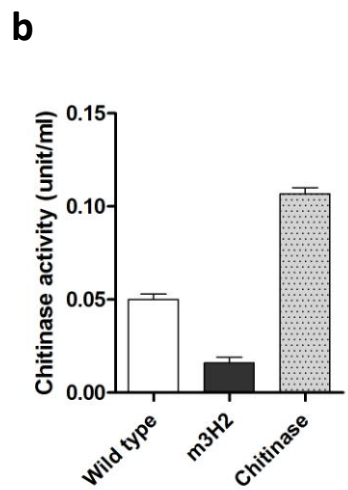
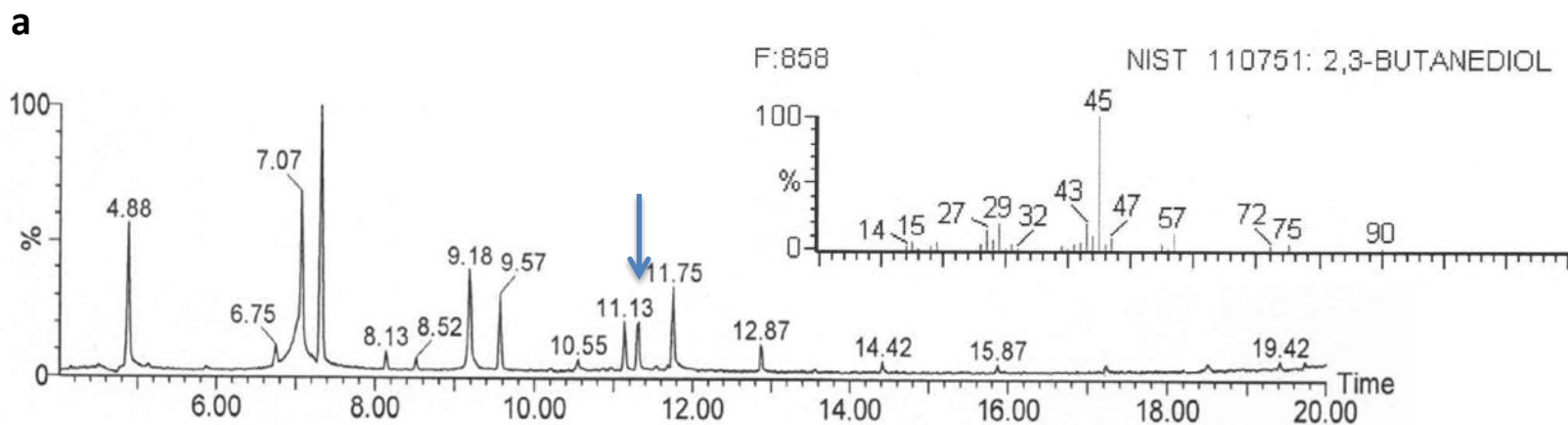


Figure S7



Supplementary Table 1. Taxonomic classification of finger millet bacterial endophytes based on 16S rDNA sequences and BLAST analysis

ID (Genbank Accession)	Tissue source	BLAST analysis	% of max. identity	Length of aligned sequence
M1(KU307449)	Roots	<i>Enterobacter</i> sp. (CP015227)	99	646
M2 (KU307450)	Seeds	<i>Pantoea</i> sp. (FN796868)	99	701
M3(KU307451)	Seeds	<i>Burkholderia</i> sp. (KC522298)	99	587
M4 (KU307452)	Shoots	<i>Pantoea</i> sp. (KT075171)	95	751
M5 (KU307453)	Shoots	<i>Burkholderia</i> sp. (KP455296)	99	586
M6 KU307454	Roots	<i>Enterobacter</i> sp. (KU935452)	99	586
M7 (KU307455)	Shoots	<i>Burkholderia</i> sp. (HQ023278)	100	644

Supplementary Table 2. Effect of endophyte strain M6 isolated from finger millet on the growth of diverse fungal pathogens *in vitro*.

Target fungal species	Diameter of growth inhibition zone in mm		
	Nystatin (10.0 U/ml)	Amphotericin (250 µg/ml)	M6
<i>Alternaria alternata</i>	0.0±0.0	0.0±0.0	0.0±0.0
<i>Alternaria arborescens</i>	0.0±0.0	0.0±0.0	0.0±0.0
<i>Aspergillus flavus</i>	2.0±0.2	0.0±0.0	3.6±0.2
<i>Aspergillus niger</i>	0.0±0.0	2.0±0.0	0.0±0.0
<i>Bionectria ochroleuca</i>	2.0±0.2	0.5±0.2	0.0±0.0
<i>Davidiella tassiana</i>	1.5±0.2	0.5±0.3	0.0±0.0
<i>Diplodia pinea</i>	2.5±0.2	3.0±0.2	0.0±0.0
<i>Diplodia seriata</i>	3.0±0.2	2.0±0.2	0.0±0.0
<i>Epicoccum nigrum</i>	0.0±0.0	0.0±0.0	0.0±0.0
<i>Fusarium avenaceum</i> (isolate 1)	2.5±0.3	3.0±0.6	1.8±0.2
<i>Fusarium graminearum</i>	1.5±1.6	0.0±0.0	5.0±0.3
<i>Fusarium lateritium</i>	0.0±0.0	1.0±0.2	0.0±0.0
<i>Fusarium sporotrichioides</i>	1.0±0.2	1.0±0.2	2.8±0.2
<i>Fusarium avenaceum</i> (isolate 2)	0.0±0.0	0.0±0.0	0.0±0.0
<i>Nigrospora oryzae</i>	0.0±0.0	0.0±0.0	1.83±0.2
<i>Nigrospora sphaerica</i>	0.0±0.0	0.0±0.0	0.0±0.0
<i>Paraconiothyrium brasiliense</i>	0.0±0.0	0.0±0.0	0.0±0.0
<i>Penicillium afellutanum</i>	3.0±0.2	3.0±0.2	0.0±0.0
<i>Penicillium expansum</i>	2.0±0.2	5.0±0.2	4.9±0.1
<i>Penicillium olsonii</i>	1.5±0.3	3.5±0.3	0.0±0.0
<i>Rosellinia corticium</i>	2.0±0.2	4.5±0.3	0.0±0.0

Supplementary Table 3. Suppression of *F. graminearum* disease symptoms in maize and wheat by endophyte M6 in replicated greenhouse trials.

Treatment	% Infection (mean ± SEM)*	% Disease reduction relative to <i>Fusarium</i> only treatment	Average yield per plant*	% Yield increase relative to <i>Fusarium</i> only treatment
Greenhouse trial 1 in maize				
<i>Fusarium</i> only	33.69±2.3	0.0	41.77±1.4	0.0
Proline fungicide	23.10±2.0	31.4	50.9±1.2	21.85
M6	10.13±0.9	69.93	39.58±2.6	-5.2
Greenhouse trial 2 in maize				
<i>Fusarium</i> only	85.11±4.5	0.0	7.8±1.1	0.0
Proline fungicide	41.42±4.5	51.33	40.8±1.2	423
M6	6.9±0.9	91.89	34.70±2.7	344
Greenhouse trial 1 in wheat				
<i>Fusarium</i> only	51.8±6.3	0.0	10.5±2.6	0.0
Proline fungicide	31.70±2.6	38.8	10.9±1.3	3.8
M6	41.1±2.6	20.6	10.6±0.8	0.95
Greenhouse trial 2 in wheat				
<i>Fusarium</i> only	54.0±2.6	0.0	17.7±1.5	0.0
Proline fungicide	31.5±4.1	41.6	20.1±2.1	13.5
M6	30.7±3.6	43.1	21.1±1.3	19.2%

*SEM is the standard error of the mean.

Supplementary Table 4. Reduction of DON mycotoxin accumulation during prolonged seed storage following treatment with endophyte M6.

Treatment	DON content (ppm) (mean ± SEM)*	% DON reduction relative to Fusarium only treatment*
Greenhouse trial 1 in maize		
<i>Fusarium</i> only	3.4±0.4	0.0
Proline fungicide	0.7±0.4	79.4
M6	0.1±0.0	97
Greenhouse trial 2 in maize		
<i>Fusarium</i> only	3.5±0.3	0.0
Proline fungicide	0.1±0.0	97.1
M6	0.1±0.0	97.1
Green house trial 1 in wheat		
<i>Fusarium</i> only	7.6±0.3	0.0
Proline fungicide	0.5±0.1	94.6
M6	1.5±0.6	81.33
Green house trial 2 in wheat		
<i>Fusarium</i> only	5.5±0.7	0.0
Proline fungicide	1.3±0.9	76.3
M6	2.0±0.4	63.6

***SEM is the standard error of the mean.**

Supplementary Table 5. Complete list of strain M6 Tn5 insertion mutants showing loss of antifungal activity against *F. graminearum* in vitro.

ID	Gene prediction	Swarming assay	Motility assay (mean ± SEM)*	Presence of flagella (%)	Biofilm (mean ± SEM)*
Wild type		+++	4.2±0.3	70%	0.8
<i>ewa-1B3::Tn5</i> <i>ewa-4B8::Tn5</i>	Transcription regulator, AraC	---	0.6±0.02	50%	0.11±0.00
<i>ewy-1C5::Tn5</i> <i>ewy-5D2::Tn5</i>	YjbH outer-membrane protein	++	0.5±0.03	10%	0.3±0.08
<i>ewm-2D7::Tn5</i>	4-hydroxyphenyl acetate 3-monoxygenase May catalyze production of phenylacetic acid (PAA)	---	0.8±0.05	20%	0.07±0.00
<i>ewpR-5D7::Tn5</i>	Transcription regulator, LysR	---	0.5±0.03	30%	0.18±0.01
<i>ewb-9F12::Tn5</i> <i>ewb-7C5::Tn5</i>	Fatty acid biosynthesis	---	0.6±0.05	30%	0.3±0.11
<i>ewvC-4B9::Tn5</i>	Colicin V production	+	1.8±0.30	60%	0.6±0.05
<i>ewT-15A12::Tn5</i>	Transport permease protein Within operon for biosynthesis of P-amino-phenyl-alanine antibiotics (PAPA).	+	1.5±0.00	30%	0.6±0.04
<i>ews-1H3::Tn5</i>	Sensor histidine kinase	+	0.8±0.16	50%	0.8±0.2
<i>ewc-3H2::Tn5</i>	Chitinase	---	1.0±0.00	20%	0.4±0.15
<i>ewfR-7D5::Tn5</i>	Transcription regulator, LysR	+	1.5±0.20	50%	0.3±0.08
<i>ewgS-10A8::Tn5</i>	Di-guanylate cyclase	---	0.8±0.30	40%	0.1±0.01
<i>ewh-5B1::Tn5</i>	Hig A protein	+++	1.6±0.30	30%	0.6±0.10
<i>ewa-8E1::Tn5</i>	Hypothetical protein	++	2.3±0.40	20%	0.5±0.09

*SEM is the standard error of the mean.

Supplementary Table 6. M6 wild type nucleotide coding sequences (Ettinger et al, 2015) corresponding to Tn5 insertion mutants that showed loss of antifungal activity against *F. graminearum* in vitro

ID	Gene sequence
<i>ewa-1B3::Tn5</i>	<p>gtgaataccattggcataaacagcgagcccatcctgacgcacagtggcttagcattaccgccgatacc actcttgccgcagacaggcaactatgacgttatctatctctcctgccctgtggcgcaatcctcgtgcagtggc agacaacagcctgaactcctggcatggcttagcgaacaggcggcgcgaggaccgccatcgcggcc gtcggaacgggctgctgttctggcggaatcgggattgctcaacgggaaaccgccaccaccactg gcactactcaaacagttctcgcgtgactacccaacgtaaaattacaaccaaaccatttctcagcgag gccgataatattactgtgcccagcgtcaaagccctctcagatctgacctccatttcacgaaacgat atacgggaaacgtgtagccacacatacccaacggaccttttccatgaaattcggagtcagttgatcgc cagtgttacagtgaagaaaacaaaccatccggatgaagataattgtcaaatcaaatctggataaaa gccaaactgcgctcggatataatccatgaaaatcttgcgatatggctggcatgagtttgcgaactttaa cgccgtttaaaatgccaccgatataatccccctgcagatattataaccgccagaattgaatccgcat gacaatgtgcaatcccaatctgagcattcaggagattgcaatgctggggatcaggatattgc gcacttaatcgccagtttaagcataaaacaacggtttcaccgggggattaccgtaagaccgtccgggc aaagatgttagtcataa</p>
<i>ewy-1C5::Tn5</i>	<p>atgaaaagaacctatctctacagcatgtggcgctctgctgagtgccgctgcatgcagaaacgat ccggcaccattggcccgtctcagtcagacttcggcggcgctgggttgctgcaaacgccaccgcgcg atggcgcggaaggggaaattagccttaactaccgtgataacgatcagatcgttactactcggcgtcgg tgcagctgttcccgtggctgaaaccacgctgcgctacaccgacgtgctgacgaaacagtaacagcagc gtgatgcttcccggcgaccagacctacaagataaagccttcgacgtcaagctgcgctgtgggaa gagagctactggatgccgacggtgtccgtggcgccaaagatacgggtgaccggctgttggatgctg aatacatcgtggccagtaaaagcctgggggcccgttcgacttctcgtcggcctgggatggggctaccgg gcaactggcgtaacgtgaaaaatccgttttgcctcagcagataaatactgctaccgcgataacagcta taagaaagcgggtccatcaacggtagaccagatgttccacggcggcatcgtgttggcggcggtgga gtatcaaacgccctggcagccattacgcctgaagctggaatatgaagggaatgactactcgcaggactt cgccgggaagattgagcagaagagcaagttaacgtcggcgccattatcgcgtcaccgactgggccc acgttaacctcagctacgagcgcggcaacaccgtagtgggttcacgctgcgaccaactttaaagca tatgcgccacactacaatgataacgcgcgcccctgcataaccagccggagccgcaggatgcgattctgc agcactccgtgtggcaaacagctgacgtgctgaaatacaatccggcctggcggatccgaaat caggtgaaagcgatacgtgtacgtgaccggcgagcaggtgaaataaccgcgactcgcgcgaaggg atcgaacgcgctaaccggatcgtaatgaacgatctgcgggaggggacccgacgatccgcgtgacgg aaaaccgccttaacctgcccaggtgacgacggaaacggacgttccagcctaagcgccatctgga aggtgaaccgctcggcatgaaaccgagctgggtcaaaaacgcgtagaaccgatcgtgcccggagac caccgagcagggctgtatatacgacaaatcgcgcttcgatttccatcagatccggctgtaaccagctc gtcggcgggcccggaaaacttctacatgatcagctggcgctatggcgacggcggatctgtggcttacc gaccacctgctgaccaccgtagcctgttcggcaacatcgtaataactacgacaagtcaactacacc aaccgcctaaagactcacagctccgcgctgctgactcgcgtgctgtaatacgtgcagaacgatg ctacgtgaataacctgcaggccaactattccagtaactcggcaatggcttctacggccagggtgacggc gggtatctgaaaccatgtacggcggcgggggcggaagtgctttatcgtcctgtcagcagcaactgg gcgttcggggtgatgcaactacgtcaagcagcgtgactggcgacgagcgcaggacatgatgaagt caccgactacagcgtcaaacgggcatctgaccgcctactggacgccctcgttcgcgctgacgtgct ggtgaaagccagcgttggctcagctacctggcggcgataagggcggtacgctggatctctaaacactt cgacagcggcgtcgtggggcggtatgccaccatcaccacgittcgcggacgaatacggggaa ggggacttcaccaaggggtctacgtgctgattccgctggatctgtctcgtcaggcccaaccgcagcc gtcggcagtaggctggacggcgtgacgcgtgacgggggtcaacagcttgacgtaagttccagctg tatgacatgacgagcgataagaacattaactccgctga</p>

<i>ewm-2D7::Tn5</i>	atgaagcctgaagagttccgcgctgatgccaacgcccgttaaccggcgaagagtatttaaaagcct gcaggacggctgagatttatctacggcgagcgctcaaagacgtcaccaccaatccggcatttcg caacggggcgctccatcgcgagatgtacgacgctgcacaagcctgacatgcaggacgctc tgctggggcaccgacaccggcagcggcgctatacccacaagttttccgctggcgaaaagtccga cgacctgcccagcagcggacgcatcggcagtggtcgcgctgagctacggctggatggggcgc acggcggactaaaagcggcttggctgctgctggcgaaccggccttctacggccagttcga acagaacgcccgttaactggtacacgctcattcaggaaccggcctgtacttaaccagccatcgtaa cccggcgtcaccgtcacaagcggcgagcgggtgaaagacgtctacatcaagctggagaaag agaccgacgcccggattatcgtcagcggcgcaagtggtagccaccaactccgacctgaccacta caacatgatcggctcggctcggcaggtgatggcgaaaaccggactcgcgctgatgtcgtcgc gccgatggatgccgaaggcgtgaagctgatctcccgcctcttacgaaatgggtgagggcgaaccg gatccccgtacgactaccgctcaccagcggctttgatgagaacgacgcatcctggtgatggatcacgt gctgatcccgtgggaaaatgtgctgatctaccgcatctcgaaccgctgctgctggacgatggaagg cggtttcgcggtgatcccgctgacggcctgctgctggcggtgaagctcactcatcaccgcc ctgctgaagaaatcccggagtgaccggcaccctggagttccgcggtacaggcggatctcggcga agtgggtggcctggcgaacatgttctggcgctgagcagctcattgttccgaagccaccctgggtc aacggcgctatcgcggatcacgcccgcctgcaaacctaccgctgatggcgccgatggcctacgc caagatcaagaacatcatcagcgtaacgtgacgtccgctgatctacctgctccagcggccggg atctgaacaaccgcagatcgaccgatctggcgaatacgtgctggctccaacgggatggtacac gtcgaacgcatcaagatttgaagctgatgtgggatgcatcggcagcagatttggcggtcgtcagagc tatacgaatcaactactccggcagccaggtgatgacccgctgagtgctcgcaggcagcagagc tccggcaacatggacaaaatgatggcgtggtcagcctgcatgtccgaatcagaccagcagcgt ggaccgtaccgcacctgcacaacaacagcagatcaacatgctcgaacaagctgctgaaatag
<i>ewp-5D7::Tn5</i>	atggactaaccagctgaaatgtttaacgcccgcgctgacgggcagcatcaccaggcggcgca gaaggtgcatcgcgtgccgtccaacctgacgaccgcatccgccagctggaagccgatcttggcgtg agctgtttatctgagaaccagcgtttgccttatctcccggggcataactcctcgtcactacgaggc agatcctgcctgtggtgatgaagcgcgatggtcgtcgggtgatgagccgaggggtatttgcct cggcgcgctggaaagcaccgcccggctgctcattcccgaacgctggcgcagtttaaccagcctat ccgcgcatcagtttgcctttctaccggccttccgggacgatgattgatggcgtactggagggcacctta agcggccttctgacggggccgctgctgacccggagctggagggcatcgggctaccgggaag agatgatgctagtcacgctcggggcacgaggtgacgcgccaagcaggttagcggcagcga cgttacgcatctcgcgaactgctcgtaccgtcgcacatctggaagctggttcatgaggacagacca cgctggccgcatcagatgagatggagtctaccacggcatgctcgcctgctcattggggcggggca tcgctgatcggcgctcgtgctggagatgctcgggacatcaggtgaagcctggccgctgg cggaaaactggcgtggcttacaacctggtggtggtggcggcgggcgatgacccggcagctgga agctttatagcgtgctaaacgaacgtctcaaccagcgccttctcataa
<i>ewb-9F12::Tn5</i>	atgcccgaaaatcatcaggaagcgcgtgggagcgttttgcggagattacgtaatgcgaaacgga atgtattgtacgacagcaaagggagcagaacgctaggccagctatcactccgtatcccgcatttt taccttcgacaaaaccagacagctgctcctgcccgggtatcgtctgacatccttctgatcgcacgttctc cggggcatttacccttccggtagcggaaaacgatctggctttttacagtacacctcgggttcgacgg gcttccgaagggcgtgatgggtgacctatggcaacctggtggccaactcgcgatgccattaccgcttttc ggccatcacagcgaagccggggcagatctggctcccattttcatgatatggggctgattggcggg ctactgcagcccgtttggcgcattcccctgctgggtgatgctgcccagatgtaataaaaaatcccctta actggctaaaatatttctgactatcaggcgaacacctccggcgccctaatttcgctacgatctgtgc gtgcaagattggcagagagcaagttgaggcattagatcttctcgtgggatgtggcttttgcggcgc agagccgattcggcccacgctacagcagtttagcgaacactttgcgcccagggatttgcggccc gcgctcctgcccgtacggcatggcggaaccacgctcactcgtcaccgggatggagaaaggaca agggctccgcttccgacgagggcggtagcgtgagctgaggcaggctcgcggataccgaggtgc gatcgtcgtcccgatcggcagcggcttctgctgatggtgagagcggggaaatggtcgtgctgctc gacgcttgcggcagatactgggacaatgacgcccacacgcaaaccttccaggccttctgctgctg gccatccgaccccgtggctgctgagcggcgatggttttctccagtccggccatttctgctgctg acgactcaagagctgctgattatcaacggtcagaacctaccgacggatattgaagagcagatcc

gccaggccgatcccgcgctggcgggaagcgacggttgctgtttgccagtgaagacgagcgcccggtt
gcgctgtgagctgatgacgcgccataaaaacgatctcgatatggcgacgctggcaccgtccgtgacc
gcgcggtggcggagcggcacggcatcacgtggatgaactgctctgtcggcgaagggcaattc
cccgaccaccagcgggaaactacagcgcacccgcgaaagcgatgaccagcagggaaacct
ggaagtagcctggcgcagctgccaggacgctcgaaacctgtgaactcgggggaaacccacc
cgctgtggcggcgtgatagccgggataatcagcagcgcgatgaacacgacgatcggcgaatcca
gtgggacgagcgcttaccggcttggcatgagctctcgcaggcgggtggcggtgattggcgagctgaa
cagcggctgggcccgcgagctctctcccgcgctgattatgactacccaccatcaatcggctggcggcc
gcgctggggcaacccgctgcccggccggctcagctcagccgtcgggagagcgccattgcccgtg
attggcatcggcgtggagctgcccggacatagcggcgtggaggcgtgtggtcgtcgtcgcagcagg
ccacagcagcaccggcgagatcccggcgcaccgctggcgtacctcgtcccttgacggtttaaccgtaa
aggcagtttctcgacgaggtcgacgcgcttcgacgcaggctacttcggcatctctcccgtgaggccgtct
atatgatccgcagcatcgtctgtgtagaaacggttcaacaggcgttaaccgatgcccggccttaaggc
gtctccctgcgcggtagcgatacggcggcttctgtgggatcagcgcacgactacgcgctggcctgc
ggcgataacgtctcggcctacagcggcttaggcaacgcgcacagatcgcggccaaccgaattcttat
ctttatgattaaaaggccaagcgtcggcgcagacaggcctgttctctcgcgtggtggcgatagagg
ggcaatgcagagcctgcgggcccggacggtgctcgtcggcattgccggaggcgtaactcggcgtgac
gccacattgcaaaaagtctcaccgaagcccagatgctggccccgcagcggcgggtgaaacacctgc
acgcccgcgcggtggctatgttcgtggcgaagggtggtggcgtcgtggtgctaagccgttcaaggc
gctggcggatggcgatcgggttatgccacgctggtggcgagcgcggtgaatcaggcggcggcgcg
aacggcattaccgcgcaaatggccatcgcagcaggcggctacctcaggcgatggcggacgccc
gggtggacagcgcagcattgactatacgaagcgcacggctacgggaaccgcgctggcgatctgatt
gaatatcaggcgtggaagcgggttggcggaccgaaaaagaccgcacctgtccagggtgggttcgat
caaaaccaacattggccacctgagggcggcggcggtgctggcggtgaaaacgtctctgatgc
tgcactccggcaatacgtacctcacctcaatttcagcagaaaaaccgcataattgcggcgattagccgt
catgttgaggtagcggcgcgcagcctgcctcatggcatgccgatggcgaagcgcgctatgcggcggt
aagcagcttggctcggcgggtaccaacggctatgtatttgcgcagcgcgccagcgggtgaaaaacg
ccaggagcccgtcgcgcgcacggcctgtctcgtcggttccatgataaagggcggttacccctcag
cgggaggcggcaaaaagggttatcgcagctccaggagagcgatattgccacctggtgctggcgtggt
gaaacccgctacgacgcggcccgcctatcgcggcgtggcgtatggcgcggatcgtcccagctggcg
gaaagccttgcgcagctcaccgtctgaagggtgggtaaagcccagccccaggctggctctcccggg
gcagggcacccagcaaatcggcatgggtgcccagctgtatcacctatcggcactatcgcacccaggt
ttgacgcgctggcgacgactattcagcagcgtatcagattgatattacgcaggcgtgtttgccgtgac
gacagctggcagcgtcgcgccagaacgtcagctctcattattgctgtagctacgcgctgtctcagag
cgtgatgcagttcggcccgcgtccggcgtccgtaatggggcacagcctgggagagtagctgcggcgg
ttatcgtggctatctcgtgagcagcggcgtggcaatggtcatcagcgcgctgttgatgtcagccc
tgacgcaggaagggcgatggcgtcgtctcagcggcgaagccgacgtccgtcagatgattccccct
ggacgggcgacattgatattgccgattcaacacgcgcgacattgaccaccatcgcaggcagtcgggcg
gcgattgacgcctgcctcaggccatcttcaaaaggcggtcacgccagaaaaataaaactgccagc
gcatttactctcgtgatgatccgatcctcggcgcctggcgcgagtggtggtcaacaacgtcacct
caccgcgggacgatcccgtttacagcaacctgaacggtagggcgtgcgaccgcaccgacgcggac
tactggaccggcaaatcgcagcccgtgagttcctcaggggcgtgcaaacgctgctggcacagggt
gagttcaccttatcgatctgagcgcggcgggttcgctgggcaaatgtgaccgcaactgaccgcccgtca
ccgggtgctggcgcaggcgcacggcgcagatgagtaacaatcactgctgacgctgctgggtacgctgt
ggcagcaagggcacgacatcaactggagcgggctgtaccacgcgaccacgcgggaggcgtaacc
ctgcccgcctaccagttctgcgcaaacgttactggctggcgggtgagacgccagcgcagaccccatct
gcaaaagaggacgctatgtcaaatcaacaccatttagccgctgaaataaaagcgattattgccggtttct
tgaggcggatcccgcgcttgacgactctcgtcggctcctggaaatggggcggactcgtggtgctg
ctggatgccatcaataaccattaaagaccgcttggcgtagccatcccggcgcggcgctgtttgaagac
tcaatacgttgacgcgggtgatcggatagtgtgggagcagcgcagccggcggctcgtcaccacc
ccggaaaccgcccgtggcggcacagcctgtcgcggcaccgcagggtaccagcaggccgggtgcct
gatacggttcaggatctgattcccgcagctggagctatgtcccagcagctaaattgttcaacggcag
ggcgcaggctctcccgatccagccgcacccgcgacgcccggacgtatcgcgctcgcggcctcgtg
gccccagccacccggtgaaggccagcgcgcacaacagctggfttaaaaagagaccaaaaagggt
ctccctcggcgtgagcgcgaccagcatctggcgcactcaccgaacggtttgtcgataaaaacgggcg
ggtcaaaacgcaatgccagcaataccgcgctgctcgcggataaccgggctctcgcggccttctgt

	<p>cagatctgctttacctccgcttfcgcatatgtggatcaccggccgtacgatgatggcaaggcgattat cgccgggatggcggcagcgcacatcgcatctcagctatgttcaactggcgctgaaccgaaaatcat gggctggccctaacgccgtgatcgccgctgctgttggcttcgggatcgtgctggctggcggtgga aaccggctggatgtaccgcccgtcgaaggccaggtacactactggtgggtggctgggaaatgttat cggctcagcatcctggcgtacttctggacgatctccccggcgtggccacgagctgggataaggt caacctgctgagcaccttcggccccctggcgccctgctggtcacctacgcccctgctggtgctttt actggtgtcgacagagaaacgcttctccgcccgaagtgttaaacagaaaccaggagaatg ctgcatga</p>
<i>ews-1H3::Tn5</i>	<p>atgacgagccgtaaacctgccatctttactggtgatgacgatcccgggctgttaaagctgctgggat gctgctggtgagtgaaggctacagcgtgacccgcaaagcgggctggagggtgaaagatcctc accgcgagaaaatcgatctggtgataagcgacctgcgatggacgaaatggatggcctcagctgtt cgcgggatccagaggcagcagccgggatgcccgtgatcattctgacggcgcacgggtgatcccg gatgcggttgcggcagcagcagggggtcttcagcttctgaccaagccggtggacaaagacgctg gtataaggctatcgacagcgcgtggaacatgcccggcggggatgaaagcgtggcgggagtc catcgtcaccgcagccccattatgctgctctcctgaacaggccggatggtggcgcagctccgacgtc agcgtgctcatcaacggccagagcggaaaccgggaaagagatcctggcccaggcagtcataacgcc agcccgcgagtaaaaatgctttatcgccattactgcccgcgcttccggaacagcttctcgaatctg aactgttggctatgcccgggcgattcaccggcgcggtgagcagtcgggaaggcgtgtccaggcg gcggaaggcggcacgctgttctggacgagatggcgacatcccgcgctgagctgagctcagctgct gctgctgattgaggagcgaaggtcggcctgggagcagcaaccgcatcgaatgaatgctgctgca ttattccgcccaccgagcttgcctgcaaaagtgtggcccgaacgagttccgaaagatcttacta ccgtctgaacgtggtgaatctgaagatccctgctgctggcgagcgcgagcgaagacattccgctgctg gaatcatctctgcccaggcggccgatcgcataaaccttggcgcgcttccaccgacgcatga agcggctgatggccgaggctggccgggtaacgtgcccagctggtgaacgtgattgagcagtgctg gctgacctcctcaccggtaacagcagatgctgtagagcaggcgtggaaggagaaaaacagg cgtgcccagcttgcggaagcgcggaatcagttcagctgaactatctgcaagctattgcagatca ccaaaggcaacgtgaccacgcccgcgcatggccggacgcaaccgaccgagttctacaagctgc tgtcgcgccacgagctggaagcaaacgattttaagagtaa</p>
<i>ewc-3H2::Tn5</i>	<p>atgaacaaaagaacattactcagtgcttatttgcggcgcatgtgtgacccgttattgctcaggcaacc ctgctgaggccagcagcgaaccttaccccttaaggccagcagatctgcagaagaaagagcaggag ttaaccaactcccgtgatggctcgggtgaagtcaacctccgacgctggacaacagcctggtggaa caaattgagcctgtaaatcgacaaccgggaaacgtaagcgcgtggaaggattatcaaggcca gagactgggattatcttcccactgctgcccggaaatatactacagcaacttctgaaagcgtgctg aaattcccggcactgtccagacctataccgatggtcgtaacagcagatgcatctgcccgaagctctg caacctgttcgagcacttcgagcaggaactggcggccagagctcctggctccggaagcggagtg gctgagcagcgtggttacgtgctgagatgggctggagcgaaggtcagaaggcggatataacggc gaatgaaccggatgtctggcaggggagacctggcggtaagacaagatggcgatctcgt tagctatttggccggtgcaaacagctctcctataactacaactacggcccgttctgaaagcagatga cggcagcgtccgctactgctggacaaacctgagctggtggcggacacctggctgaacctgcttccg gatcttcttctgcctaccgcagccgcaaaaccaagcagctgctgaggtatcgacggcacatggca gccgaacgatcacgataaggcgaatggtctggtaccgggctcggagtgaccacgcagatcatcaac ggcggcgtggagtgtggcggcccagctgagatcgccagctcaaaaccgtatcaaaactacaag agttcgcaactacctgaaagtgcctgttccgttaacgaagtctgggctgcgcaacatgaagcagtt cgacgaaggcggctggtgcccgtgaagatctactgggaacaggactggggatggagcgcgggatac cccgtcaggccagacctacttccagctggtgggtaccagacgccattcagcgcctttaaaggggt gactacaccaaagtgcgtgaagcatttctcaatgtgaacgtggtgggtgaagcgggacttccgacggc ggtagcgtcacgcaagccccgagcccagcccctgctgacccaacggacgaaggcaacaccacggc ggtgcccagacgataaacccccgctccggacgataatacggcagcgggtaaacctgcaagcgggt agcaaaaatcgggctccgggtgggtgaggtgaaagcgggtaaacagtttctgaaacgctgctgctg accgacgaagacggttaaccacctgactataacctggacggctccgaacggccagaccgtaagcggc gaagataaagcattattacctcaatgcgcccgaagtggcagcggcgcagcagctaccgatcaacct taccgtcagtgagggcagctgagcagcaccaccagctatacgtgaaactgacgggtaagcagacc aacggcggccagaccgggacttaccgacctggacctcaaaaccaaatggaaagcagggcagatc</p>

	gttaacaaccgcgccagctgttccagtgcaaaccctatccgtacagcggctggtgcaataacgcgcca tctactacgagccaggtaaagggtgcatggcaggacgcgtggactgcgctgtaa
<i>ewf-7D5::Tn5</i>	atgatgaatcttttacactggcgtgctggttgcctggccgatccagtaataatttcccgtgccgctgaag aggcggatgacgcagtcaggtgccagccaggcagtcagtcagttagaggcctcattaggattgctggt attcacgcgagagcgacgccacatcggcgtgactgccctggcgagcgggttgcaagaagcaag gagtatgctggcggctggatccatccgtgactggcggatgagagccgggggctgagcggcgga cgcattcgtctgcccagtttctcgtgacatccacgttttggccgggctgctgcgcgactaaagcgcct gcatcctgaaatcgaggtggtcgtcctgaaggcagcggaccaggaggtcgaagagtggctggcggca gatacggttgatctgggctggtcatgaaccctgtcccggcgctgtaagcgaatcttagggcaggatg catgggtcgtggtgtgacagccagtcaccgtcaggctcgtatacagtcagcggcgcacccctga ggaactggcagaccagccctcgtgctcgaaccggcgggtgcgccgtcaatggaaaaagcctgatgg aacaggctggcctcagctgctgacgtgcgggtgaccgtccgcgactggatcagcgcctgctgctg gtgcgcgaaggcatggcgctgcgctgatacctgaatccgccctgccgatgaattacgcggttgtgc gtcgtacccgtgacgcctcgtgctgcccggaaattgggtggtatgttcgaggtgggcaaatatcccg cgcgacgcaggcgttattagaagggtgctcaaaatgaaaaggctgcgctga
<i>ewg-10A8::Tn5</i>	atgaccacaacatttctcagaaatagggtgtgcatgaacaaaagttgtcatctcagcctgcggtttt acgtccagggatctgctgttcttaaccagtaacggaatacaggcttcgcatattcattttagtgggatg aggcatcgcaacaggatagaaaaatacctataaatcagaatgctcatgttgggttctcggaaaa ggtatcttaagtctcctggagacctgaagcagctggcgtccgtgctcaatgcgttggccttattcgacgc gtcacgctgtatggcgacataccggatggctggtatatacgcaccctgggcagctctttaaataatagttat caattatcattgactgactagcccgcgttccggatgctcactggttctcagccaccatcattttaa ggaacgttcgactattacgcgatcgtcagggataattctcgaagacaacgtcaagtggtaaca aaaagagagattgacgttttataaattctaccgcggcatgtccgtaaaagaaatgicgatgaaatgg gactatctaataaaacggtttatacccaccgtaaggaaggcgtgctgaaattacgcttaattaagcggtg gctacacgattcgcaaatatcaatgcggaaagaatcaagcggcggagtcacaaacacggaattt acggataaggaaagcagagattttaaagcattatataaaaaagagatcttccctgctatcagatcattacc gatcgtgacaaaaaggcgttaggctttgagatactgatccgctggaacaaaaacggtaaaattgtcaa gccgaccagtttctcagcgtatattcaaatcagatagattggtgaaaattaccgcgctagtattcatgcc gccgtgctgggaattaataagtataatgtaataactattttctgtaatttccacctgcctggcctccgg aaatgcattgcctgatatggaaggaaagctatcgacatgctgctcaaaccgcagtgggccgagaagc tggctttgaattcgagaagatattgacgtgacgaaggacaaagggatcccagaaacctgcggcatt tgcgtaatacaggggtgctgattttctggatgactgcttctaatcaccacacatgttcccggctgaggca ggtgcattttgatggactcaagctggatcgggatcgttgagcattttgggcaaacgacaatgactataa cctgatcaaagcgatacagattatagcagatgaccggaacggactgtattgcagagggagtagaca gtgaggaaaaattgaaaaattagtcgcgctggcgctcaaaaacttcagggatatttattcgcgagcc gtgaaagaggacgagttggtcagatggtcagaatttttagttaa
<i>ewh-5B1::Tn5</i>	Atgacactcaacaggcactccgcaaacccaccacgccggcgacgtgttgcagtatgagtatcttgaacc gctcaatctgaaaatcagcagatctggcggagatgctcaatgttaccgcaacaccatcagcgcgctggtca ataacaatcgaacttactgcccgatatggcagatcaaacctggcaaaagccttgataaccagattgaatttgg ctgaacttacagctgaacgtcagatctgggaagcgaatctaactccaggactcaggaggagctaaagccg tataaagaccgttgcggaagtattggctaagcgaatctggccagccggatgttgcctga
<i>ewa-8E1::Tn5</i>	gtgatccgcaaagagaaagggcgcgtggatgctatggcgaccgcttccgcgacgtgctcagct gacgccgctgctgctcaggttgacgctatatacagcaaccgcaagcggatggaacagaccg caatggagattgcgagcgtgtgaaaacgtcggatgccacgggtgctccgcgcallcaggcgtgggtt cgccgggctgctgcatcctaagcaaacgctggagcagtggttggctccgggtgctcacctccagcgaaa agatgtccactacggtgaatacgtcgcagcagctcaacgcgagcattgattcgtgctggaggggc atcagcacacctgcgaggtttatccgagccccacaaccgctacgcaatggcccaggcggctctctgct tggcgcaggcagggcaggtcgcataattggcattggcgcctccggcattctggccgagatataccgca ggctgtcagccgatgggttaccgccacgcgcttaaccgtaccggaatagggttccgagcagc tgattgcgctcagcgcggcagctgctggtgatgatggcgcagaaatccgcgacccgggaggggca aacacgcctgcgtgaagcaaacgctgggcatccaccatctgctgaccaacgcctcagttcgc gttccagcaaggaggccagcgtggtgatccacgttccgcgaggcggcaaaaaggcaaaattccgct

	ccacggcacggtgctgctgtgtctggagatgatcattttatccgtcgctccaccgagccgcagcgcacc atcaagtcgatgaagcgcatcaacgagttacaccgtgggttaaagccggggaagaaaagtacctaa
--	---

Supplementary Table 7. Gene-specific primers used in quantitative real-time PCR analysis.

Gene ID	PCR primers
ewpR	5D7F: 5'- GGCATAACTTCCTGCGCTAC - 3' 5D7R: 5': CAGTACGCCATCAATCATCG - 3'
ewpF1	PhzF1F: 5'- TTTTCTCACCGGGCGTTTC- 3' PhzF1R: 5'- GTATGTGCGGAGCCGGTAA- 3'
ewpF2	PhzF2F: 5'- AAATGGCGCAGCAGCATAA- 3' PhzF2R: 5'- GTCGGTGCGCACGAAAA- 3'
ewfR	D5F : 5'- GGGGACAGTAACGACGAAAC - 3' D5R : 5'- CGGCAATCTGTCGATATGAA - 3'
ewfD	FusE/MFPF: 5'- TGGCCGTGCGGGATAAT- 3' FusE/MFPR: 5'- GGATCGATGGTGTAAGCACATC- 3'
ewfE	FusEF: 5'- CGTCGAGCCCACCTTTAGC- 3' FusER: 5'- TCCGGCAATCTGTCGATATG- 3'
ewgS	A8F 5: GGAGTCAAAACACGGAATTTACG - 3' A8R 5: ATCTGATAAGCAGGGAAGATCTCTTT - 3'
ewvC	B9F 5: TGTTTTATGCTTAAACTGGCGATT - 3' B9R 5: CGAATGCGGTGGGATATCA - 3'
16SrDNA (housekeeping gene)	799F: 5'- AACMGGATTAGATACCCKG- 3' 1492R: 5'- GGTTACCTTGTTACGACTT- 3'